STATUS OF LATTICE FIELD THEORY AND COMPUTER SIMULATIONS

Akira Ukawa

Institute of Physics, University of Tsukuba
Ibaraki 305, Japan

Abstract

Recent development in the study of lattice field theories with computer simulations is surveyed. The status of lattice QCD calculation of the hadron mass spectrum, various weak matrix elements and the nature of the finite-temperature phase transition to the quark-gluon plasma phase is discussed. Recent studies on the Higgs boson mass and scalar-fermion systems are reviewed. Projects for building dedicated computers are briefly touched upon.

1. Introduction

Lattice field theory is a fairly recent terminology for studies of quantum field theories defined on a discrete space-time lattice. The cornerstone of this field is the formulation of quantum chromodynamics on a lattice by K. Wilson in 1974.[1] His formulation elucidated how gauge fields at strong coupling naturally lead to quark confinement. It also provided a theoretical framework for calculating the properties of hadrons starting from the basic QCD lagrangian of quarks and gluons. The application of computer simulation methods marked another major step in the development of lattice field theories.[2,3] This method yielded evidence[3] for the first time that the lattice cutoff could be successfully removed to define continuum QCD with the confining property. The first computer calculations of the hadron mass spectrum that immediately followed[4,5] demonstrated the practical feasibility of extracting the continuum predictions from lattice QCD through numerical simulations.

Spurred by these initial successes and helped in an essential way by the remarkable development of computer technologies, an enormous amount of theoretical and numerical work has since been made. This has brought substantial progress and considerable widening of the scope of lattice field theories. The mass spectrum of hadrons and the nature of the finite-temperature QCD phase transition[6,7] have been subjected to an increasingly detailed scrutiny. In addition there have been serious attempts to extract a wider variety of strong interaction observables from lattice QCD, notably a number of phenomenologically important weak matrix elements of hadrons.[8,9,10] Lattice studies have also been extended to gauge theories including scalar fields which are of relevance to the electro-weak sector of the standard model and possibly beyond. A key observation here is that the triviality of self-couplings of scalar fields (*i.e.*, the renormalized couplings vanish as the ultraviolet cutoff tends to infinity) should lead to an upper bound on the Higgs boson mass within the standard model.[11,12] The triviality of $O(n)$-symmetric scalar field theories has been established a few years ago[13], and the numerical value of the bound within the approximation of ignoring the gauge fields and fermions has been derived.[13,14,15] More recently effort is concentrated on scalar-fermion systems, in particular on the problem of incorporating chiral fermions into a lattice framework. In another direction lattice studies of QED and other non-asymptotically-free field theories have been started.[16] There are also some lattice simulations of the baryon number violation in the standard model.[17] Finally we should note that the lattice formulation coupled with numerical simulations is not limited to standard field theories. Indeed it has been applied to random surfaces[18] in the hope of acquiring better understanding of quantum gravity and strings.

In this review we attempt to survey the development in lattice field theories and computer simulations since the time of the last High Energy Conference at Munich. Before going into the survey let us briefly recall the essential features of the lattice approach.

The basic quantity in quantum field theory is the Green's function or the vacuum expectation value of products $\mathcal{O}(\phi)$ of field operators $\phi(x)$. For a given action $S(\phi)$, this quantity can be represented by the Feynman path integral,

$$< \mathcal{O}(\phi) >= \frac{1}{Z} \int \prod_x d\phi(x) \mathcal{O}(\phi) e^{-S(\phi)}, \qquad (1)$$

where time is rotated into the imaginary axis and Z is the normalization factor so that $< 1 >= 1$. The integration over the field $\phi(x)$ at each space-time point x gives rise to ultraviolet divergences which have to be regularized. In the lattice theory this is done by replacing the space-time continuum by a discrete set of points forming a regular lattice and placing fields only on the lattice. Indeed if a is the lattice spacing between a pair of nearest-neighbour lattice points, the momentum cannot exceed the value π/a. If one further restricts the lattice to be of a finite extent, the lattice path integral (1) becomes a well-defined finite-dimensional integral which allows numerical as well as analytical treatments.

Methods for extraction of physical quantities in lattice theories parallel those in the continuum. For example the mass m_ϕ (in units of 1/a) of a particle created by a field ϕ, be it elementary or composite, can be determined from the exponential decay of the two-point function for a large time separation,

$$< \phi(t)\phi(0) > \stackrel{t\to\infty}{\longrightarrow} \frac{Z_\phi}{2m_\phi} \exp(-m_\phi t), \qquad (2)$$

where Z_ϕ is a wave-function renormalization factor. Similarly the three-point function can be used to find the matrix element of an operator $\mathcal{O}$ between the particle states $|\phi_1>$ and $|\phi_2>$ of a mass m_1 and m_2;

$$< \phi_1(t_1)\mathcal{O}(0)\phi_2(t_2) > \stackrel{t_1\to\infty, t_2\to-\infty}{\longrightarrow}$$
$$\frac{\sqrt{Z_1}}{2m_1} e^{-m_1 t_1} < \phi_1|\mathcal{O}|\phi_2 > e^{-m_2|t_2|} \frac{\sqrt{Z_2}}{2m_2}. \qquad (3)$$

Evaluating the path integral (1) is generally a formidable task. If coupling constants are small one can use the well-known weak-coupling perturbative expansion which reduces the problem to integrations of Gaussian type. However, this method ceases to be applicable when coupling constants become large or if the dynamics is not analytic around zero coupling. The computer simulation provides a method for a direct numerical estimation of (1) which may be applied irrespective of the magnitude of coupling constants. In this method an ensemble of configuration of fields is stochastically generated with the distribution proportional to $\exp(-S(\phi))$ so that the average over the ensemble gives the vacuum expectation value;

$$< \mathcal{O}(\phi) >= \lim_{N\to\infty} \frac{1}{N} \sum_{c=1}^{N} \mathcal{O}(\phi^{(c)}). \qquad (4)$$

The existence of fermions in nature present a technical complication in numerical simulations. Fermions are represented by anti-commuting Grassmann numbers in the path integral, which can not be directly manipulated by electronic computers. This problem has been overcome by the invention of the algorithms[19] in which the Grassmann integration problem is replaced by that of inverting the lattice Dirac operator. As a result simulations including fermions have become quite common recently. However, because the lattice Dirac operator is a large matrix with its dimension often exceeding 10^6, fermion simulations are much more computer-time consuming compared to purely bosonic ones by a factor of $\mathcal{O}(10^3)$ and more.

There are certain conditions that have to be met in a meaningful simulation. Clearly the number of configurations has to be sufficiently large so that the statistical error can be controlled. Furthermore the lattice spacing a and the linear extent of the lattice La should satisfy the inequality

$$\frac{1}{La} \ll m \ll \frac{1}{a}, \qquad (5)$$

with m the typical energy scale of the system being simulated. The right-hand side represents the condition that the ultraviolet cutoff be large compared to the physical mass scale. In more geometric terms this means that the lattice mesh should be fine enough to well approximate the continuum space-time when viewed in units of the physical length scale $1/m$. The left-hand side states that the lattice size has to be larger than this length scale, violation of which will clearly introduce distortions in the dynamics of the system.

These conditions place a severe demand on the computing power needed for lattice field theory simulations. In a hadron mass calculation, for example, it is natural to take $m^{-1} \sim 1$fm, the typical hadron radius. For $a \sim 0.1$fm one then needs at least $L \sim 20$ for the lattice size. This means over 10^7 integration variables from the gauge fields alone, and this number increases $2^4 = 16$ fold for a doubly large lattice. Furthermore inclusion of fermions results in a dramatic increase in the amount of computations. It should be no wonder that the progress in lattice simulations depended critically on the increase of the available computer power. In fact the demand for more power has quickly outpaced the development of commercial supercomputers even though it has been recording a ten-fold increase in speed every 4-5 years. The trend born from the desire to overcome this impasse is the building of special purpose computers dedicated to lattice simulations. Among a number of projects[20-25], the computers built by the Columbia[21] and APE[23] groups have already produced physics results which have contributed much to the recent development, and the construction is close to completion in several other projects.[22,24,25]

We now turn to the survey of the recent progress. In Sect. 2 we discuss the hadron mass spectrum. The weak matrix elements of hadrons and the finite temperature QCD phase transition are discussed in Sect. 3 and Sect. 4. The recent refinements in the Higgs boson mass bound and the studies of scalar-fermion and other theories are described in Sect. 5. Section 6 contains a summary and an outlook.

2. Hadron mass spectrum

The calculation of the mass spectrum of hadrons is the basic problem in lattice QCD. The primary purpose is to verify that QCD with its specific non-perturbative dynamics at low energies quantitatively explains the experimental spectrum. At the same time one likes to extract predictions on exotic states such as glueballs and multi-quark hadrons.

Simulations for the spectrum can be divided into two categories, quenched and full QCD, depending on the treatment of the quark degrees of freedom. In the former only valence quarks are kept, while sea quarks are also taken into account in the latter. Empirically the OZI rule and the success of quark models suggest that the quenched approximation may be resonable for flavor non-singlet hadrons. This is an assumption, however, whose validity should be either confirmed or disproved through dynamical calculations in lattice QCD.

Table 1 illustrates the typical values of lattice parameters used in the recent spectrum calculations. We note that the quark mass m_q is not yet realistically small, and consequently meson masses are mostly restricted to the range $m_\pi/m_\rho \geq 0.5$, *i.e.*, above the $\rho \to \pi\pi$ threshold. This is due to the fact that the inversion of the lattice Dirac operator, needed at various stages of simulations, slows down as $\mathcal{O}(1/m_q a)$ in computer time and that the fluctuation of observables increases simultaneously.

2.1. Prediction of nucleon mass

In lattice QCD simulations the experimental values of several hadron masses have to be used as input to fix the quark masses which are *a priori* not known. For the up and down quark, assuming that they are degenerate, their common mass may be fixed by demanding that the pion to ρ meson mass ratio takes the experimental value $m_\pi/m_\rho =$ 140MeV/770MeV=0.18. The nucleon to ρ mass ratio is then predicted, which can be compared with the value $m_N/m_\rho =$ 940MeV/770MeV=1.22 in the real world.

A large number of simulations has been made to evaluate this ratio since the first calculation in 1981.[4,5] In spite of the effort the results remained very unsatisfactory even in the quenched approximation till quite recently. Indeed the quenched values published before the end of 1988 were not only high compared to the experimental value but also scattered over a wide range $m_N/m_\rho \sim 1.3-1.5$ with large errors of up to 10-15%, which made it difficult to recognize a systematic trend in the data. The full QCD results were even worse giving $m_N/m_\rho \sim 1.4 - 1.7$. (See [26,27] for a compilation of data up to this period.)

Three groups[28,29,30] recently reported improved quenched results which have substantially clarified the confusing status. The improvement comes in part from the use of a larger spatial lattice (24^3 compared to $16^3 - 18^3$ or smaller previously) and generally higher statistics, which reduce statistical errors and allow calculations at smaller quark masses. Equally important is the development of the technique of extended hadron operators[32,28] and wall sources[30] for enhancing the signal of ground

Table 1: Recent hadron mass spectrum calculations. KS and W stand for staggered and Wilson quark action, g the coupling constant and N_f the number of flavors. The inverse lattice spacing a^{-1} is estimated from the ρ meson mass. The quark mass m_q and ratio m_π/m_ρ show the smallest value reached. The data of [31,46,47] became available after the Conference.

	ref.	action	size	$\beta = \frac{6}{g^2}$	a^{-1}(GeV)	m_q(MeV)	m_π/m_ρ
quenched							
APE	[28]	W	$24^3 \times 32$	5.7	1.45(2)	32	0.43
	[28]	KS	$24^3 \times 32$	5.7	0.88(3)	9	0.33
Iwasaki *et al.*	[29]	W	$24^3 \times 60$	5.85	1.86(7)	40	0.53
APE	[28]	W	$24^3 \times 32$	6.0	2.30(9)	39	0.50
	[31]	KS	$24^3 \times 32$	6.0	1.80(15)	18	0.51
Gupta *et al.*	[30]	KS	$24^3 \times 40$	6.0	1.93(10)	19	0.53
full QCD							
HEMCGC	[44]	KS($N_f = 2$)	16^4	5.6	1.6(1)	16	0.49
MT$_C$	[48]	KS($N_f = 4$)	$16^3 \times 24$	5.35	1.11(6)	11	0.36
Gupta *et al.*	[45]	W ($N_f = 2$)	16^4	5.4–5.6	1.6–2.4	60	0.7
Columbia	[46]	KS($N_f = 2$)	$16^3 \times 32$	5.7	1.95(2)	20	0.56
Fukugita *et al.*	[47]	KS($N_f = 2$)	$16^4 - 20^4$	5.5–5.7	1.3–2.4	20	0.6

state hadrons in hadron propagators.

In Fig. 1 we show the new data for hadron mass ratios. The filled and open symbols signify the use of the Wilson or the Kogut-Susskind (staggered) quark action, which are the two formulations of lattice fermions commonly used. The APE data for the staggered action at $\beta = 6.0$[31] were reported after the Conference. The cross at lower left of the figure is the experimental point and the one in the middle right represents the limit of infinite quark mass. The solid lines indicate the behavior expected from models: the one on the right is based on a quark model mass formula including hyperfine splitting[33], and the one on the left is the prediction of the first-order chiral perturbation theory.[30]

In order to see the significance of this figure we recall that the continuum limit of lattice QCD is to take the lattice spacing $a \to 0$ and simultaneously to let the coupling constant $g^2 \to 0$ ($\beta \equiv 6/g^2 \to \infty$), namely the lattice spacing a decreases for a larger β. For the Wilson quark action the data in Fig. 1 (filled symbols) taken at $\beta = 5.7-6.0$ therefore show the trend that the curve of m_N/m_ρ becomes lower and closer to experiment as the lattice spacing decreases. For the staggered action (open symbols) there is discrepancy between the results of the two groups at $\beta = 6.0$ [30,31], which should be clarified. A decreasing trend of m_N/m_ρ also appears to hold, however.

The trend can be illustrated in a different way. In Fig. 1 we plotted the hadron mass ratios for each quark mass value at which the simulation was made. Alternatively one can extrapolate the hadron mass data obtained at several quark masses to the experimental point $m_\pi/m_\rho = 0.18$, form the ratio m_N/m_ρ from the extrapolated values, and plot it against the inverse lattice spacing estimated from the ρ meson mass through $a^{-1} = 770\text{MeV}/m_\rho a$. The result is given in Fig. 2 where we added previous data [34] for a smaller a and the analytic estimates in the

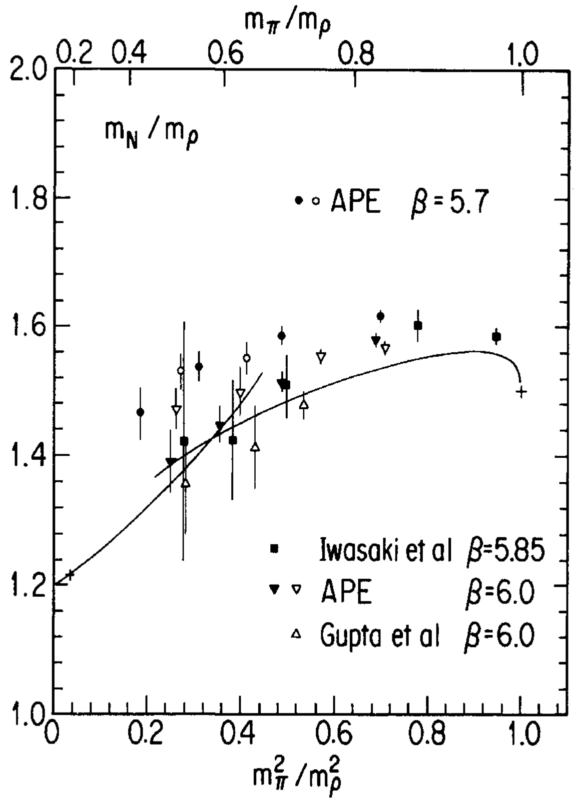

Figure 1: Recent results for m_N/m_ρ as a function of $(m_\pi/m_\rho)^2$ on a 24^3 spatial lattice in the quenched approximation. Filled and open symbols are for the Wilson and staggered quark actions. Data are from APE[28,31], Iwasaki *et al.*[29] and Gupta *et al.*[30]. For the meaning of crosses and curves, see text.

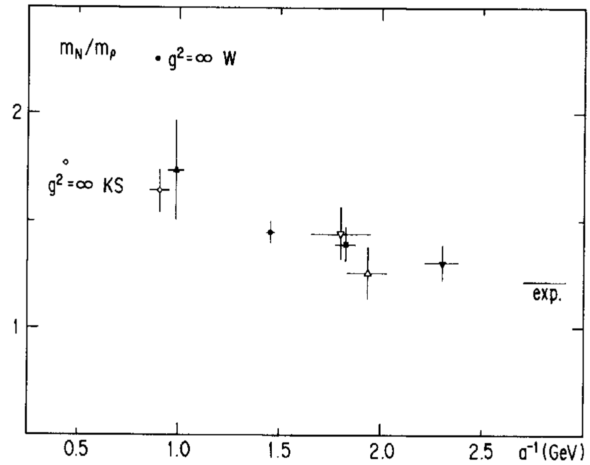

Figure 2: m_N/m_ρ as a function of the inverse lattice spacing a^{-1} in the quenched approximation, Extrapolation of hadron mass data in the quark mass was made using $(m_\pi a)^2 = A \cdot m_q a$ and $m_H a = B \cdot m_q a + C$ for $H=$ nucleon and ρ with A, B and C constants. The data are from [28-31] except for the analytic estimates at $g^2=\infty$[35,36] and the filled triangle at $a^{-1} \sim 1$GeV.[34] The meaning of symbols is the same as in Fig. 1. The horizontal bar at right represents the experimental value.

strong coupling limit $g^2 = \infty$.[35,36] Clearly the ratio m_N/m_ρ is a decreasing function of the lattice spacing, and its value $m_N/m_\rho \sim 1.3$ around $a^{-1} \sim 2$GeV is fairly close to the experiment one.

It is also worth noting that the ratio obtained with the two lattice fermion actions, which is quite different at $g^2 = \infty$, becomes reasonably consistent below $a^{-1} \sim 1$GeV. This supports the expectation that the two actions represent an equivalent way of discretizing the action in the continuum.

2.2. Scaling in the quenched approximation

We expect that hadron mass ratios become constant toward the continuum limit $a \to 0$. Figure 2 suggests that for the m_N/m_ρ ratio in the quenched approximation the constant behavior may become approximately realized below $a \sim 0.1$fm (this lattice spacing corresponds to $\beta \sim 6.0$).

A more stringent check on the approach to the continuum limit is provided by the scaling law predicted by the renormalization group. It states that a physical quantity $\mathcal{O}$ of a mass dimension ℓ should behave as,

$$\mathcal{O} \sim \text{constant} \cdot \Lambda_L^\ell, \tag{6}$$

as $a \to 0$ and $g^2 \to 0$ where

$$\Lambda_L = \frac{1}{a}(b_0 g^2)^{-b_1/2b_0^2} \cdot \exp(-\frac{1}{2b_0 g^2}), \tag{7}$$

is the lattice Λ parameter with b_0 and b_1 the first two coefficients of the β-function of QCD.

In Fig. 3 we plot the ρ meson mass at the physical point $m_\pi/m_\rho = 0.18$ normalized by Λ_L of the pure gauge theory as a function of $\beta = 6/g^2$ together with a similar ratio for the 0^{++} glueball mass ($m(0^{++})$), the string tension (σ) for the static q-$\overline{q}$ potential, and the critical temperature of the deconfining phase transition (T_c) (see Sect. 4.3) calculated in the quenched approximation.[37-43] According to (6) these ratios should become constant as $\beta \to \infty$. The constant behavior is not yet seen for the ρ meson mass up to $\beta = 6.0$. The behavior of the string tension σ and the critical temperature T_c evaluated at higher β suggest that the scaling behavior may set in at $\beta \sim 6.3-6.5$. Note also that the rate of decrease for smaller β is similar among the quantities. Ratios of physical quantities (*e.g.*, $m(0^{++})/\sqrt{\sigma}$) therefore show a milder variation with β than those with respect to Λ_L.

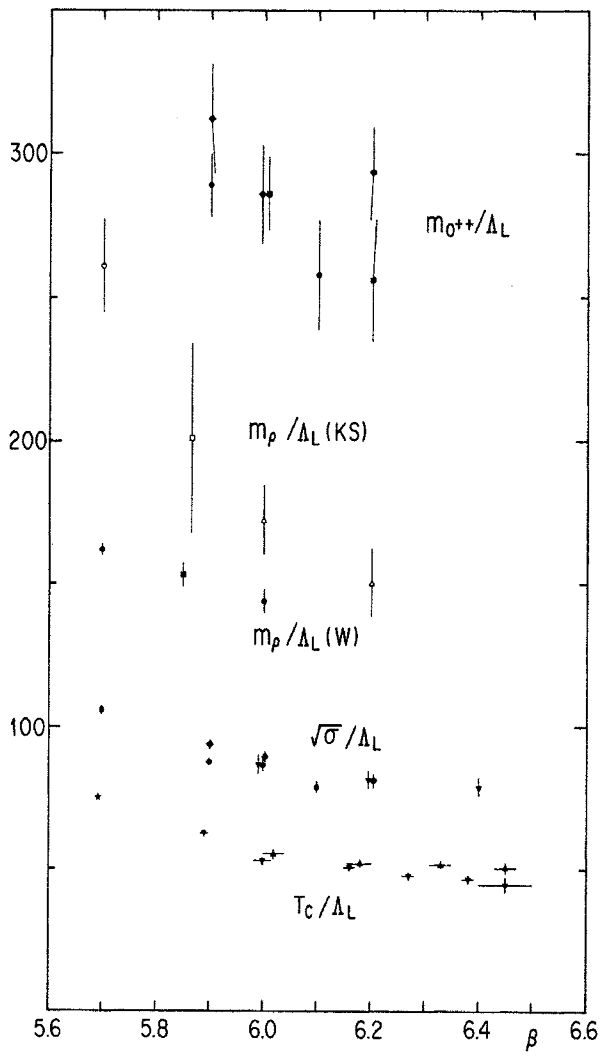

Figure 3: Scaling behavior in the quenched approximation. For m_ρ the data are from [28](circle), [29](filled square), [30](triangle) and [37](open square), and for the other quantities, from [38](circle), [39](diamond), [40](square), [41](upward triangle) and [42](downward triangle).

2.3. Full QCD simulations

We have seen that the recent studies have led to a considerable improvement in the quenched hadron mass data. They indicate that the quenched m_N/m_ρ would be reasonably close to the experimental value. It should be emphasized, however, that the two values need not exactly coincide since sea quarks are ignored. The quenched approximation may even cease to be meaningful for realistically small quark masses where the effect of decay channels such as $\rho \to \pi\pi \to \rho$ and $\Delta \to N\pi \to \Delta$, which do not occur without sea quarks in hadron propagators, has to be taken into account. Full QCD studies including sea quarks are therefore indispensable for further understanding of the hadron mass spectrum.

Dynamical fermion simulations needed for such studies take vastly more computer time than the quenched one as we have mentioned in the Introduction. For this reason the previous full QCD mass spectrum calculations were restricted to the lattice size of order 10^4 and the lattice spacing of order 0.2fm. The lesson we have learned from the recent quenched studies tells us that a high value should be expected for m_N/m_ρ with such a large lattice spacing, which indeed was the case.[26]

Since late 1988 two groups[44,45] have been running full QCD simulations on a larger lattice at weaker couplings to explore the spectrum closer to the continuum and two more groups[46,47] joined the effort recently. Another group[48] has been making attempts to study the region of small quark masses at the cost of a large lattice spacing (see Table 1). Some results are already available, and they indicate an improved behavior of m_N/m_ρ when the lattice spacing is reduced to $a \sim 0.15-0.1$fm.

An interesting question in full QCD is how sea quark effects manifest themselves in the hadron mass spectrum. On this point the simulations made to date have not seen clear deviation from the quenched results; the apparent differences observed in masses in lattice units turned out to be absorbable into a shift of the coupling constant within errors of $\mathcal{O}(10\%)$ (see, *e.g.*, [34]). This means that in the region of relatively heavy quark with $m_\pi/m_\rho \geq 0.5$ explored so far (see Table 1), the dominant effect of sea quark is a renormalzation of the coupling constant depending only weakly on length scale. Physical effects of sea quarks may not become significant until the ratio m_π/m_ρ is reduced well below the $\rho \to \pi\pi$ threshold.

We note that a resolution of the $U(1)$ problem appears to require just such a reduction. Indeed a quenched study[49] of the flavor-singlet and non-singlet pseudoscalar meson propagators indicates that the mass splitting between the two mesons becomes appreciable only if quark masses are decreased to realistically small values.

Unfortunately decreasing quark masses in full QCD simulations is not feasible at present because of the problems mentioned in the beginning of this section. A detailed study of sea quark effects in the mass spectrum has to await substantial improvement in computer power and algorithms.

2.4. Nucleon sigma term and polarized structure function

There are several matrix elements in which effects of sea quarks may be pronounced. One is the nucleon sigma term defined by

$$\sigma_N = \frac{1}{2}(m_u + m_d) < N|\overline{u}u + \overline{d}d|N > . \quad (8)$$

Current algebra and π-N dispersion analyses indicate $\sigma_N \sim 50 - 60\mathrm{MeV}$, while the use of flavor $SU(3)$ symmetry with the first-order breaking leads to $\sigma_N \sim \sigma_0/(1-y)$ with $\sigma_0 \sim 25\mathrm{MeV}$ where $y = 2 < N|\overline{s}s|N > / < N|\overline{u}u + \overline{d}d|N >$ parametrizes the unknown contribution of the strange quark in the sea. The two estimates for σ_N combined imply a large contribution of the strange quark $y \sim 0.5$. (The magnitude of the sigma term has been the subject of much discussion. See [50] for a recent critical analysis and a list of literature.)

There are two types of contributions to the sigma term; one in which the scalar density $S = \overline{u}u + \overline{d}d$ couples to a valence quark of nucleon and the other through a sea quark. The first contribution has been estimated within the quenched approximation using the nucleon-scalar density-nucleon three-point function $< N(t_1)S(0)\overline{N}(t_2) >$ as well as by the derivative $\partial m_N/\partial m_q$.[51,52] The results fall in the range 15−20MeV, and the new quenched data for m_N [28–31] yield similar values with the derivative method. This range of value is reasonably close to the estimate for σ_0 for which the strange sea quark is ignored. It would be quite interesting to attempt a direct lattice calculation of the sea quark contribution to the sigma term and see whether it explains the difference between the quenched results and the experimental estimate.[53]

Another interesting quantity is the first moment of the polarized proton structure function whose value was reported by the EMC collaboration.[54] A naive quark-parton model interpretation of the EMC result leads to the conclusion that the fraction of proton helicity carried by the strange quark is about −20% which nearly cancel the sum of that of up and down quarks.[55] It has been argued[56], on the other hand, that this conclusion does not necessarily follow if gluon contributions omitted in the naive argument are taken into account.

A lattice estimate of this contribution was recently attempted[57] within the quenched approximation with the result that it is too small to affect the quark-parton analysis. The calculation, however, was made with a heavy quark ($m_\pi/m_\rho \sim 0.8$) on a small lattice ($6^3 \times 10$). Simulations with smaller quark masses on a much larger lattice are needed for a realistic estimate. Let us note that a lattice evaluation of the quark contribution should also be made. This involves a calculation of the matrix element of the flavor-singlet axial-vector current for a polarized nucleon. Again there are sea as well as valence quark contributions, and the main question is the magnitude of the former.[53]

We add two remarks on related matrix elements. (1) For the nucleon matrix element of flavor non-singlet axial-vector currents, the sea quark contribution is absent. The matrix element has been studied within the quenched approximation[58], where a reasonable agreement with the experimental values was obtained (*e.g.*, $g_A = 1.11(12)$ as compared to 1.259(4) experimentally). (2) In [59], a method was proposed for a lattice computation of the neutron electric dipole moment D_n induced by the QCD vacuum angle θ. This angle may be chirally rotated into the quark mass matrix $m_q \rightarrow m_q \exp(i\theta\gamma_5)$. To obtain D_n for a small θ one then has to compute the neutron propagator in an external electric field with the $m_q\overline{q}\gamma_5 q$ vertex inserted. There are sea- and valence-type diagrams that contribute to the propagator, and [59] suggested to drop the former. This is not justified. Indeed it is the sea term which gives the physical value of the moment, while the term coming from valence quarks vanishes in the continuum limit.[60]

2.5. Hadron structure

The internal structure of hadrons may be examined through form factors and structure functions.

The electromagnetic form factors of pion[61,62] and nucleon[63] and a few moments of their structure functions[62,63] have been studied some time ago. These calculations were reviewed in [64], and here we only add that effort for improvement has been continuing for nucleon form factors.[65]

2.6. *Exotic states*

The glueball spectrum in the pure gauge theory has been extensively studied through numerical simulations both for $SU(2)$ and $SU(3)$ gauge groups. For small spatial volumes the spectrum can also be calculated analytically in an expansion in $z = mL$ with m the mass of the lowest gluball state and L the linear spatial size.[66,67,68] The results explain the data quite well up to $z \sim 5-6$, especially if lattice effects are taken into account.[69]

The simulation data were compiled already two years ago[70], and there has not been much progress since then. The lowest glueball state in the pure $SU(3)$ theory has $J^{PC} = 0^{++}$ and the next lowest state is 2^{++}. States with unnatural J^{PC} such as 0^{--} and 1^{-+} are either heavy or have not been seen.[39] The estimate for the masses made in the compilation[70] is

$$m(0^{++})/\sqrt{\sigma} = 3.25(21), \tag{9}$$

$$m(2^{++})/m(0^{++}) = 1.543(82), \tag{10}$$

with σ the string tension for the static quark-antiquark potential (see Fig. 3 for the scaling behavior of these quantities). If $\sqrt{\sigma} = 420\text{MeV}$ is used, one finds $m(0^{++}) = 1370(90)\text{MeV}$ and $m(2^{++}) = 2100(180)\text{MeV}$.

It should be kept in mind that the results obtained in the pure gauge theory do not take into account the mixing of glueballs with $\overline{q}q$ mesons. Studying this question requires full QCD simulations. An attempt was made recently.[71]

Another type of exotic states is multi-quark hadrons. A well-known example is the six-quark 0^+ dibaryon H predicted in the bag model[72] to have a mass $m_H = 2150MeV$ which is slightly below the $2m_\Lambda$ threshold. A quenched lattice study[29] reports that m_H is smaller than $2m_\Lambda$. The value of the mass difference $2m_\Lambda - m_H$ is not yet established, however. There is also a study of mesoniums $\overline{q}^2q^2$.[73]

3. Weak matrix elements of hadrons

Studies of weak matrix elements represent an ambitious program. Weak interaction processes involving hadrons receive strong interaction corrections. These are often estimated by various phenomenological models. Ambiguities inherent in such calculations have been one of the obstacles in resolving important issues in weak interactions such as the $\Delta I = 1/2$ rule, the value of the Cabibbo-Kobayashi-Maskawa mixing matrix and the origin of CP violations. Lattice QCD simulations attempt to make first principle calculations of hadronic matrix elements that appear in the analyses of these questions.

The initial work toward this goal was made in 1984.[8,9,10] It was soon realized that achieving this goal requires development of a theoretical framework to deal with the complicated renormalization and mixing of operators on a lattice. Substantial increase of computer power was also needed in order to use a large lattice with high statistics for reliable predictions . A large part of the theoretical framework has since been developed (see [74] for a detailed review) and the last two years saw the start of large scale quenched simulations using the framework and aiming at quantitative predictions of several matrix elements. The results and the problems that remain to be clarified will be discussed below.

Up to now almost all numerical simulations have been made within the quenched approximation using a lattice of a typical size $24^3 \times 40$ and a lattice spacing $a \sim 0.1\text{fm}$. The methods, however, apply unmodified to full QCD once gauge configurations are generated with sea quarks taken into account. There are four types of matrix elements studied, mainly for π, K or D mesons: the decay constant $< 0|J_\mu|M >$, the semi-leptonic form factor $< M'|J_\mu|M >$, the mixing amplitude $< \overline{M}|H_W|M >$ and the two meson decay amplitude $< M_1M_2|H_W|M >$.

Phenomenologically it is quite important to extend computations to B mesons. A number of recent work [75–78] addressed this problem using the technique of effective action for heavy quarks proposed in [79].

3.1. *Pseudoscalar meson decay constant*

In Fig. 4 we plot the data[80-83,75-78] for the decay constant of a pseudoscalar meson made of a light

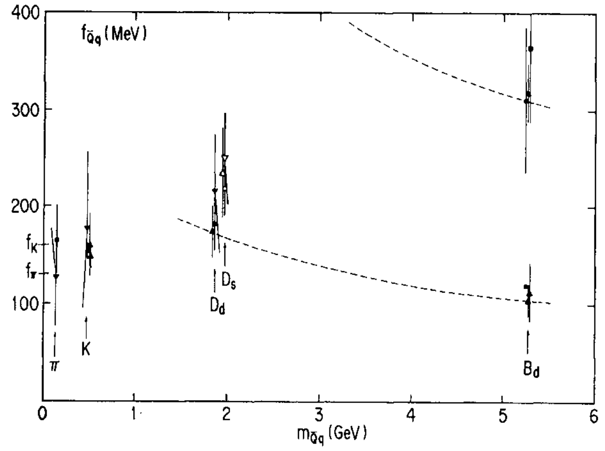

Figure 4: Pseudoscalar meson decay constant as a function of the meson mass. Data are from [80](inverted triangle), [81,82,76](circle), [83,78](triangle) and [77](square). Broken lines indicate the behavior $f_{\overline{Q}q} \sim (m_{\overline{Q}q})^{-1/2}$. Recent data at upper right are obtained[76-78] by the method of effective action for heavy quarks.

quark q and a heavy quark $\overline{Q}$ as a function of the meson mass $m_{\overline{Q}q}$. Up to charmed mesons the data [80-83] are not new. They indicate $f_{D_d} \approx 180$MeV and $f_{D_s}/f_{D_d} \approx 1.2$. It is certainly desirable to improve these estimates for charmed mesons and also those for pions and K mesons.

A calculation of the B meson decay constant presents a technical problem in that lattices with $a^{-1} \sim 2$GeV presently used are obviously too coarse for the bottom quark with the mass $m_b \sim 5$GeV. The previous work[82,83] bypassed the difficulty using the scaling law expected to hold for large values of the heavy quark mass m_Q,

$$f_{\overline{Q}q} \sim \frac{1}{\sqrt{m_{\overline{Q}q}}}, \tag{11}$$

and made extrapolations from the results obtained in the region of charmed mesons. This procedure gives the data points at lower right in Fig. 4.

Alternatively one can derive an effective action for heavy quarks in an expansion in $1/m_Q$ and use it together with the usual action for light quarks to numerically simulate B mesons on a lattice with a lattice spacing $a > m_b^{-1}$.[79] This method has recently been tested.[75-78] The results for the B meson decay constant f_B are unexpectedly large compared to those of the first method as shown in Fig. 4 (upper right data points).

There are several possible sources for the discrepancy which should be examined. The use of the first method requires the D meson to be in the region satisfying (11), which is not yet established. The results for the D meson decay constant obtained at the inverse lattice spacing $a^{-1} \sim 2$GeV should themselves be checked by simulations with a smaller lattice spacing. In the second method only the leading term in $1/m_Q$ has been computed, and the magnitude of the next-order correction is not known. The wave-function renormalization factor for the current, estimated perturbatively[84,85], is generally modified by non-perturbative corrections. Each of these factors may not be large, but they may accumulate to a significant correction in the results obtained with the two methods.

3.2. Form factors for semileptonic decays

Semi-leptonic decays of D and B mesons give important information on the flavor mixing matrix. For an extraction of the mixing matrix from the experimental decay rate, form factors of weak currents have to be supplied. Two groups[86,87,88] have been testing the lattice methods on K and D decays as a preparation to treat more interesting B decays.

For $D \to K\ell\nu$ decays the current matrix element $< K|\bar{s}\gamma_\mu c|D >$ is parametrized by the two form factors $f^+(q^2)$ and $f^0(q^2)$. Computing the matrix element at several values of the momentum transfer q and assuming the pole dominance $f^{+,0}(q^2) = f^{+,0}(0)/(1 - q^2/m_D^*)$, the two groups reported $f^+_{D\to K}(0) = 0.88(15)$[86] and $0.66(9)$[87,88], to be compared with the experimental value $0.79(5)(6)$ obtained by assuming $|V_{cs}| = 0.975$ where the first error is statistical and the second systematic.[89]

Quite recently one of the groups[88] calculated the decay form factors for the $D \to K^*\ell\nu$ transition. For the three form factor that appear in the matrix element $< K^*|\bar{s}\gamma_\mu(1-\gamma_5)c|D >$, they found $V(0) = 0.85(8)$, $A_1(0) = 0.52(7)$ and $A_2(0) = 0.05(35)$. The values reported by the experiment E691 at FNAL[90] are $0.9(3)(1)$, $0.46(5)(5)$ and $0.0(2)(1)$, respectively. The agreement is intriguing, especially for A_2 for which phenomenological models[91] tend to give a value $A_2(0) \sim 1.0$.

Table 2: K meson B parameter at the scale of the inverse lattice spacing in the quenched approximation. The first error is statistical and the second systematic(if available). Use of the Wilson or the staggered quark action is indicated by the symbols W and KS. New data are underlined. The data at β=6.4[95] became available after the Conference.

$\beta = 6/g^2$	$10^3 - 12^3$	16^3	18^3	24^3	32^3	action	ref
5.7	0.91(11)					W	[92]
		1.00(10)(12)				W	[93]
		0.98(2)				KS	[94]
6.0	0.81(16)(6)					W	[81]
		0.83(11)(11)		0.67(8)(4)		W	[93]
		0.70(2)		0.70(1)		KS	[94]
6.1	0.76(20)(21)					W	[93]
6.2		0.88(20)(28)				W	[81]
			0.69(3)			KS	[94]
6.4					0.53(5) †	KS	[95]

† preliminary

3.3. B parameter

The K meson B parameter is defined by

$$B_K = \frac{<\overline{K}|\bar{s}\gamma_\mu(1-\gamma_5)d \cdot \bar{s}\gamma_\mu(1-\gamma_5)d|K>}{\frac{8}{3}f_K^2 m_K^2}, \quad (12)$$

where the denominator is the vacuum saturation value. A precise determination of the parameter allows to constrain the mixing matrix and the top quark mass through the CP violation parameter ϵ. The B parameter defined above is not renormalization group invariant. The invariant quantity is given by

$$\hat{B}_K = B_K(\mu)(\alpha_s(\mu))^{-2/(11-2N_f/3)}. \quad (13)$$

In Table 2 lattice results for B_K obtained by three groups[92,93,94,95] are tabulated according to the spatial lattice size and the coupling constant $\beta = 6/g^2$. The data underlined are new, and the one on an 32^3 lattice at $\beta = 6.4$ is a preliminary result [95] which appeared after the Conference. Two of the groups[92,93] use the Wilson quark action, and the third group[94,95] the staggered action. Smaller errors in the results of the third group is due to the fact that the staggered action possesses an $U(1)$ chiral symmetry, which is enough to protect the left-left four-quark operator in (12) from mixings with operators of left-right chiral structure[96], while the contribution from such operators exist in the Wilson case and have to be non-perturbatively subtracted.[92,93] The results for the two actions show reasonable agreement within the errors.

A better estimate of B_K is expected for a larger spatial size and a smaller lattice spacing (*i.e.*, larger β). At the time of the Conference the best result in these respects were those at $\beta = 6.0$ on a 24^3 lattice, which indicated $B_K \approx 0.7$ at the scale $a^{-1} \sim 2$GeV. It was important to check this result by simulations on a lattice with a smaller lattice spacing since there is a 30% decrease in the value of B_K between $\beta = 5.7$ and 6.0. This check is being carried out at $\beta = 6.4$ on a $32^3 \times 48$ lattice. A preliminary result for the staggered quark action[95] is listed in Table 2, which shows a further decrease at the level of 20 – 30% between $\beta = 6.0$ and $\beta = 6.4$. The decrease over $\beta = 5.7 - 6.4$ suggests the presence of a term proportional to the lattice spacing a with a sizable coefficient in the B parameter. If one converts the three data[94,95] for B_K at $\beta = 5.7, 6.0$ and 6.4 into $\hat{B}_K$ using $\Lambda_{QCD} = 150\text{MeV}$ and $\mu = 1/a$ with $N_f = 3$ and extrapolate linearly in a toward the continuum limit $a \to 0$, one finds $\hat{B}_K \sim 0.6$ at $a = 0$. For comparison predictions of theoretical models range from 0.33[97] from the lowest-order chiral perturbation theory, 0.33(9)[98]–0.55(25)[99] from QCD sum rule to 0.66(10)[100] using the $1/N_c$ expansion.

The value of the B parameter is also needed in the discussion of the B-$\overline{B}$ mixing. Previous studies[82,83] on the meson mass dependence indicated that it saturates to the vacuum-insertion value $B \approx 1$ beyond the region of charmed meson masses. Recent calculations[75,76] using the effective action for heavy quarks found results consistent with $B = 1$ for B mesons.

Finally we note that a full QCD evaluation of the B parameter is in progress[95] using the gauge configurations generated by the Columbia group.[46]

3.4. $K \to \pi\pi$ amplitudes

A number of attempts have been made to calculate the $K \to \pi\pi$ amplitudes in order to understand the $\Delta I = 1/2$ rule[101,81,102,92,93,103] and to constrain the CP violating angle in the mixing matrix through the parameter ϵ'.[103,104,105] As a testing ground of the lattice methods, somewhat simpler $D \to K\pi$ amplitudes are also studied.[106,107] The early calculations made prior to 1988[101,81,102] (see [74] for a review) revealed substantial difficulties in a lattice evaluation of the $K \to \pi\pi$ amplitudes which have not been overcome by the recent studies[92,93,103].

Technically the difficulty arises from the fact that the $\Delta S = 1$ four-quark operators relevant for $K \to \pi\pi$ decays generally mix with a number of operators including those of lower dimension, whose contributions have to be subtracted away to find the physical amplitude.[108,96] For the Wilson quark action there is a special kinematical point ($m_d = m_s$ and all mesons at rest) where none of the extra operators contribute.[101] One may make calculations at this point and extrapolate the result to the physical point using chiral perturbation theory. Chiral perturbation theory also relates $K \to \pi\pi$ amplitudes to those for $K \to \pi$.[109,108,96] Hence the former could be estimated from the latter. With this method a non-perturbative subtraction of the contributions of extra operators has to be made, however.

The results of latest calculations[92,93,103] using these techniques agree that the isospin 2 amplitude A_2 has the right sign but larger by a factor of two compared to experiment, while the isospin 0 amplitude A_0 shows statistical fluctuations too large to take a meaningful average. For the A_0 amplitude it has been suggested[102] that the presence of a scalar particle pole in the the final $\pi\pi$ amplitude may be the cause of large statistical fluctuations. It is possible that the factor two discrepancy in the A_2 amplitude is also related to final-state interactions.[110] (A large finite lattice spacing correction is another possible cause in view of the recent results for the B parameter.) These indications point toward the importance of understanding final-state interactions[111], and studies in this direction have been started.[95,112]

4. QCD phase transitions at finite temperatures

The dynamics of QCD in the vacuum are characterized by the confinement of quarks and gluons and the spontaneous breakdown of chiral symmetry. It is expected that both these properties disappear through a phase transition at a sufficient high temperature or baryon density.[6,7]

The first computer studies of QCD phase transitions at finite temperatures[113,114], made soon after the introduction of the method to lattice QCD, showed quite convincingly that the pure gauge system loses the confining property above a certain temperature. Subsequent numerical simulations carried out over the period 1981-1987[115], combined with the theoretical analyses[116,117,118], led to the following picture of the phase diagram of QCD as a function of the temperature T and the quark mass m_q : (i) the pure $SU(3)$ gauge theory at $m_q = \infty$ undergoes a first-order deconfining phase transition[116] characterized by a spontaneous breakdown of the global $Z(3)$ symmetry[7] in the high-temperature phase. (ii) As the quark mass decreases from infinity, the first-order phase transition weakens and may eventually disappear as a result of an explicit breaking of the $Z(3)$ symmetry due to finite quark masses[117]. (iii) For light quarks, however, the transition reappears. This transition becomes more abrupt in temperature as the quark mass decreases. Its basic characteristic is that the chiral symmetry, which is spontaneously broken at low temperatures, becomes restored above the transition temperature. A renormalization group analysis of the σ-model of mesons predicts that this chiral phase transition is of first order for the number of degenerate quark flavors $N_f \geq 3$, while for $N_f = 2$ it could be either of first or of second order.[118]

The potential problem with the early work that led to the above picture was the qualitative nature of analyses with small spatial lattices and limited statistics. With greatly improved computer power it has recently become possible to make a quantitative study of the nature of the phase transition on much larger lattices with higher statistics. In particular the order of the phase transition for the pure $SU(3)$ gauge theory has been subjected to detailed finite-size analyses, and similar studies are being pursued for the chiral transition in the presence of light quarks.

4.1. Order of the phase transition in pure $SU(3)$ gauge theory

In 1988 the Italian APE collaboration[119] and the Columbia group[120] applied their QCD-dedicated computers for a detailed examination of the phase transition in the pure $SU(3)$ lattice gauge system. Although the two groups both employed lattices of four time slices with similar spatial volume and statistics, their original conclusions at the time of the Munich Conference were quite different; APE suggested that the transition may be of second order in contrast to the theoretical prediction[116] and the conclusion of the previous studies, while the Columbia group found it to be weakly but definitely first-order.

The APE group concentrated their effort on the measurement of the correlation length ξ using a few new techniques in their simulation. For a second-order transition this quantity goes to infinity at the critical point, while it is expected to remain finite for a first-order transition. The APE group found that the correlation length increases linearly with the spatial lattice size L up to $L = 16$. A continuation of this trend would mean $\xi = \infty$ in the infinite volume limit. This interpretation of the data is the basis of their suggestion that the transition may be of second order.

The simulation of the Columbia group was more standard. Running a long simulation close to the transition point, they observed that physical quantities take either of the two values, one characteristic of the confined phase and the other that of the deconfined phase, and that the values occasionally make a rapid transition from one to the other as a function of the simulation time. This is taken as evidence for the coexistence of the two phases at the transition temperature, which is a characteristic feature of a first-order phase transition. The difference in the values of observables between the two phases, however, is much smaller than the previous estimates on smaller lattices. Hence they concluded that the transition is weakly first order.

The controversy was resolved[121,122] by an application of finite-size scaling methods developed in statistical mechanics.[123] As is well known, the mathematical singularity marking a phase transition occurs only at infinite volume. The finite-size scaling theory predicts how the singular behavior develops in observables as the lattice size increases and how the quantitative characteristics of this development differ depending on the order of phase transitions.

Let us take the susceptibility of an observable $\mathcal{O}$ defined by $\chi = V \cdot (< \mathcal{O}^2 > - < \mathcal{O} >^2)$ with V the lattice volume. The maximum value of the susceptibility χ_{max} attained on a lattice of a linear size L generally grows as

$$\chi_{max} \sim L^{\rho}. \tag{14}$$

According to the finite-size scaling theory, the exponent ρ takes the value $\rho = d$, the dimension of lattice, for a first-order transition, while for a second-order transition $\rho = \gamma/\nu$ with γ and ν the standard critical exponents. Since this ratio generally satisfies $\gamma/\nu < d$, the value of the exponent provides a quantitative indicator of the order of the transition.

The order parameter of the deconfinement transition is the Polyakov line Ω[7], and the relevant dimension is that of space $d = 3$. In Fig. 5 we plot the data for the maximum value of the Polyakov line susceptibility χ_{max}[121,124] as a function of the spatial lattice size with the temporal size fixed at 4. Fitting the data to (14) gives $\rho = 3.02(14)$ in a nice agreement with the space dimension $d = 3$, which strongly

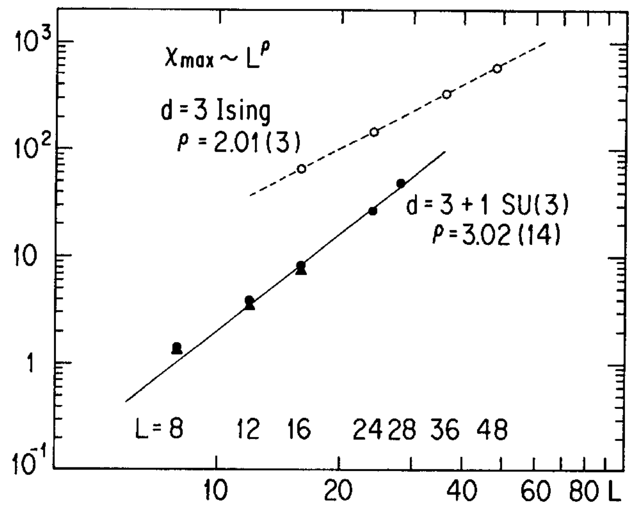

Figure 5: Spatial size dependence of the maximum of the susceptibility for the Polyakov line on an $L^3 \times 4$ lattice. The filled symbols are for the $SU(3)$ pure gauge theory obtained in [121](circles) and [124](triangles). The open circles are for the 3-dimensional Ising model with a second-order phase transition.

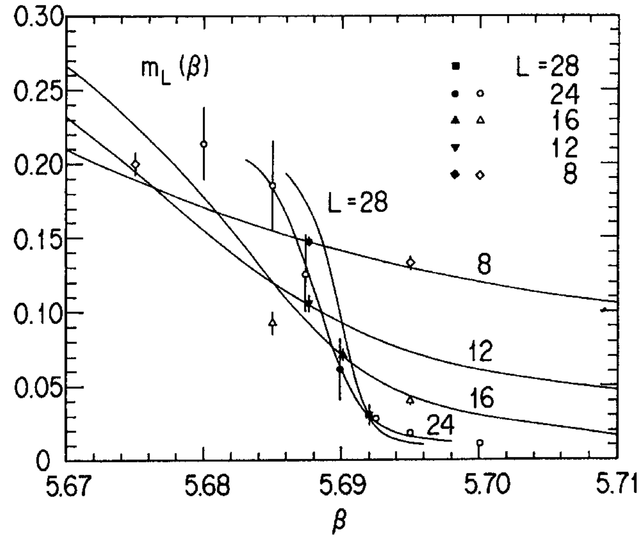

Figure 6: Mass gap on a $L^3 \times 4$ lattice for various L as a function of $\beta = 6/g^2$.[121]. Curves are obtained by the method of [125] from the data shown with filled symbols.

supports a first-order phase transition. For comparison the three-dimensional Ising model with a well-known second order transition exhibits a smaller exponent as illustrated in the figure.

The mass gap $m = 1/\xi$ (extracted from the unsubtracted correlation function of the Polyakov line) also exhibits characteristically different finite-size behaviors between the two types of transitions. Figure 6 shows the data[121] for the mass $m = m_L(\beta)$ calculated on an $L^3 \times 4$ lattice for various L. The temperature increases for a larger $\beta = 6/g^2$ and the transition point is estimated to be $\beta_c = 5.69226(41)$.[121] The curves are obtained by the method[125] which allows an extrapolation of observables away from the point where the simulation is made. One sees in Fig. 6 a clear trend toward the development of a discontinuity in $m_L(\beta)$ at β_c as the volume increases. Note in particular that the curves for different L cross each other. The behavior for a second-order case is expected to be quite different in that the infinite volume curve, which vanishes at $\beta = \beta_c$, is approached smoothly from above without crossings as the lattice size increases.[121]

It is important to observe that close to and below the transition point $\beta \approx \beta_c$ the mass m_L initially decreases with L but eventually begins to increase for a large enough L. The original APE data[119] with the largest size $L = 16$ were insufficient to observe this change of behavior as a function of the lattice size. They subsequently took data on an $L = 24$ lattice, and the result[124] confirmed the behavior. The Columbia group also reported[126] the values of m_L for $L = 24$ which are in good agreement with those plotted in Fig. 6. Thus there is now agreement that the finite-size behavior of the mass gap also supports a first-order phase transition in the pure gauge theory.

The phases of the pure gauge theory at finite temperatures are characterized by the global $Z(3)$ symmetry acting on the Polyakov line Ω which is defined at each point of space. This suggests that the dynamics of the phase transition may be described in terms of a $Z(3)$-symmetric effective theory of Ω in 3 dimensions. In fact the theoretical analysis of the order[116] is based on the assumption that the interaction of the effective theory is short-ranged. This has been confirmed by an explicit numerical construction of the effective action.[121] Furthermore a number of simulations for $Z(3)$-symmetric models[127-130], which includes the well-known Potts model, have found only first-order

Table 3: Parameters of recent work on the phase transition with light quarks using the staggered quark action. The number of flavors is denoted as N_f. For the N_f=2+1 case, the first quark mass is for up and down quarks and the second for strange quark.

	size	m_q/T	ref
$N_f = 4$	$(4^3 - 12^3) \times 4$	0.1	[133]
	$16^3 \times 4$	0.04–0.2	[135]
	$16^3 \times 6$	0.06, 0.15	[135]
	$12^3 \times 8$	0.2	[132]
	$16^3 \times 8$	0.08	[132]
$N_f = 3$	$16^3 \times 4$	0.1	[134]
$N_f = 2$	$(4^3 - 12^3) \times 4$	0.05, 0.1	[133]
	$16^3 \times 4$	0.04, 0.1	[134]
	$12^3 \times 8$	0.1, 0.2	[131]
$N_f = 2 + 1$	$12^3 \times 4$	0.05+1.0	[136]
	$16^3 \times 4$	0.1+0.4	[134]

phase transitions, and no indication of a second-order transition has been seen.

One can conclude with confidence that the deconfining phase transition in the pure $SU(3)$ gauge theory is of first order in agreement with the theoretical analysis[116].

4.2. Order of the transition for light quarks

A number of large-scale dynamical fermion simulations with the staggerd action has been carried out [131–136] during the last year to study the chiral transition in the presence of light quarks in detail (see Table 3 for parameters). The lattice size has been enlarged up to $16^3 \times 8$[132] compared to $8^3 \times 4 - 10^3 \times 6$ typical in the previous simulations, and the quark mass has been reduced to $m_q/T \sim 0.05$. For the critical temperature $T_c \sim 150 - 200$MeV (see Sect. 4.3), this ratio corresponds to $m_q \sim 7 - 10$MeV which is almost realistic.

For the system with four degenerate quarks ($N_f = 4$) there is strong evidence for a first-order phase transition for the quark mass below $m_q/T \sim 0.1$ on a lattice with the temporal lattice size equal to 4 [133,135], 6 [135] and 8 [132]. This comes from the existence of metastability signals in the simulation time history of physical quantities, which become increasingly clearer for a smaller quark mass[132,135] and a larger spatial lattice size[133], and a finite-size scaling analysis on lattices with four time slices.[133] Evidence has also been reported for a first-order transition for the $N_f = 3$ case.[134] These results are consistent with the prediction of the σ-model analysis.[118]

For the physically more important case of $N_f = 2$, extensive data[133,134] have been collected for lattices with the temporal size equal to 4. The time history of observables is quite irregular compared to the $N_f = 4$ case, and no clear sign of a coexistence of the low- and high-temperature phases has been seen in the range $m_q/T = 0.04 - 0.1$.[133,134] Visual inspection of time histories, however, can not detect the presence of a very weak first-order transition. Quantitative finite-size tests are needed to determine the order for this case.[133]

We show in Fig. 7 the maximum value of the susceptibility of the Polyakov line as a function of the spatial volume L^3 at $m_q/T = 0.04 - 0.1$. The data up to the volume 12^3 on the left[133] do not exclude an increase linear in volume corresponding to a first-order transition. The right-most points for a 16^3 spatial lattice reported quite recently[134] indicate, however, that the maximum flattens off to a constant for large volumes, suggesting an absence of a phase transition for $m_q/T = 0.04 - 0.1$.

Theoretically the transition in the chiral limit $m_q = 0$ could be either of second or of first order for $N_f = 2$. A second-order transition disappears as soon as the quark mass, explicitly breaking chiral symmetry, is turned on. On the other hand a first-order transition generally persists up to a certain quark mass $m_q = m_q^c$, beyond which there will be no phase transitions. Absence of a phase transition for a finite quark mass down to $m_q/T = 0.04$ does not yet settle the question which possibility is realized at $m_q = 0$.

A realistic finite-temperature simulation requires a strange quark in addition to light up and down quarks. With their masses in the ratio $m_s/m_{u,d} \approx 25$, this $N_f = 2 + 1$ case should be closer to the

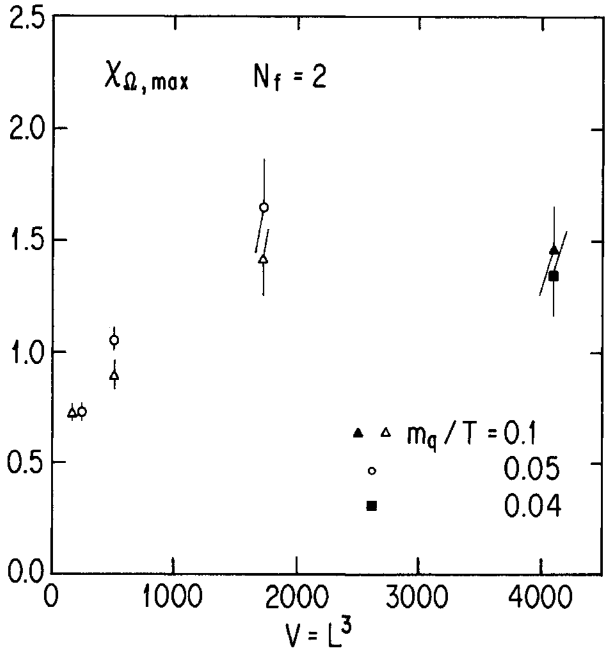

Figure 7: Spatial volume dependence of the maximum of the susceptibility for the Polyakov line for the N_f=2 case. Data are taken on an L^3x4 lattice at m_q/T=0.1 (filled[134] and open[133] triangles), 0.05(circles[133]) and 0.04(square[134]).

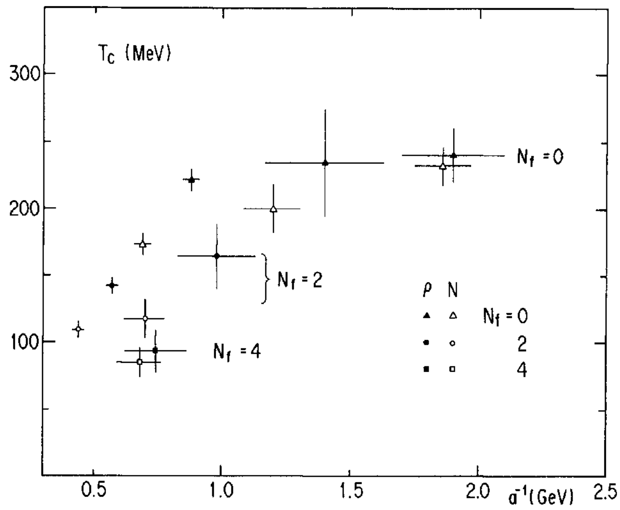

Figure 8: Critical temperature of QCD phase transition as a function of the inverse lattice spacing. Open symbols are obtained using the nucleon mass as input, and the filled ones using the ρ meson mass. Finite temperature data are from [41,42] for the pure gauge theory (N_f=0), [37] for N_f=2 and [132] for N_f=4, and hadron mass data from [28, 30, 37, 48].

$N_f = 2$ system than that for $N_f = 3$, and a recent study with $m_{u,d}/T = 0.1$ and $m_s/m_{u,d} = 4$ did not find signatures for a first-order transition.[134]

4.3. Critical temperature

Finite-temperature simulations combined with hadron mass estimates at zero temperature allows a determination of the ratio T_c/m_H with T_c the critical temperature and m_H a hadron mass. Using experimental hadron masses one can determine T_c in physical units. The critical temperature obtained by using the ρ meson or the nucleon mass as input is compiled in Fig. 8 as a function of the inverse lattice spacing for various number of flavors. The quark action is the staggered one, and the lattice spacing is estimated by the hadron mass used for that of the critical temperature. Except for the $N_f = 4$ case[132] the data are not new.

For the pure gauge theory($N_f = 0$) the critical temperature determined from m_ρ are quite constant at $T_c \sim 230 - 240$MeV, and the estimates based on m_N are converging toward these values as the lattice spacing decreases. The latter is a reflection of the behavior of the quenched m_N/m_ρ ratio discussed in Sect. 2.1. For the scaling behavior of T_c itself, see Fig. 3.

With light dynamical quarks ($N_f = 2$ and 4) the lattice spacing is still large $a \sim 0.3 - 0.2$fm, and the constant behavior of T_c necessary for a continuum prediction is not yet seen. The data show, however, that T_c for a given lattice spacing decreases with the number of flavors. Intuitively this is understandable as the color screening effect of quark vacuum polarizations weakens the confining force, and therefore it requires less thermal energy to destroy the confining property. It is possible that the transition temperature in the real world is less than 200MeV, perhaps as low as 150MeV.

4.4. High temperature plasma phase

Many investigations had already been made by the time of the Munich Conference to explore the physical characteristics of the high temperature plasma phase. The quantities examined for this purpose included internal energy density and pressure, various plasma screening length[137] and susceptibilities. Recently the surface tension of the wall separating the low- and high-temperature phases of the pure gauge system at the critical temperature has been added to the list.[138,139] We only summarize a few main points found in these investigations, referring to reviews[140] for details and literature.

The energy density rapidly rises across T_c to a value consistent with that for weakly interacting quarks and gluons over a fairly narrow range of temperature $\delta T/T_c < \mathcal{O}(10\%)$. This applies not only to the pure gauge and $N_f = 4$ systems with a first-order transition but also to the $N_f = 2$ and $2+1$[136] cases which do not have a sharp first-order transition.

The quick rise to the value expected for almost free quarks and gluons is not universal. The pressure, for example, takes a small value near the transition and rises only gradually. For all the quantities studied, however, the data is consistent with the free gas behavior once the temperature exceeds $T/T_c \sim 2-3$. The weak-coupling perturbation theory appears to describe the plasma well beyond this range of temperature. [140]

A precise determination of physical quantities close to the transition requires a large spatial lattice size and high statistics. In the pure gauge theory such a study[120] have revealed that the energy density sharply bends down below $T/T_c \sim 1.1$. As a result the latent heat on a lattice with 4 or 6 time slices is reduced to roughly half of the free gluon value. Similar detailed studies are beginning to be made for the chiral transition.[136,135]

4.5. Phase transition at high density

In the above we have summarized the results for finite temperatures. A phase transition is also expected at high density. Attempts at understanding this transition has been seriously hampered by the fact that the QCD action becomes complex at a finite quark chemical potential introduced to induce a finite density, for which the standard simulation methods fail.[141,142,143] Several alternative simulation methods have been devised[144,145,146], and it was found[144] that the chiral symmetry becomes restored through a first-order phase transition at high density. This result, however, is obtained only at the unphysical limit of strong coupling $g^2 = \infty$, and the techniques themselves are restricted either to this limit[144] or to very small lattices (*e.g.,* 2^4 or 4^4).[145,146] A Realistic study of the finite-density transition requires a breakthrough in the method of simulating systems with complex actions.

5. Electro-weak sector of the standard model

The Glashow-Salam-Weinberg theory has been extremely successful in describing the electro-weak interactions. Experimentally there is yet no sign of its breakdown. Theoretically, however, the model is far from complete. Aside from the large number of parameters that have to be fixed experimentally, it is defined only perturbatively in the continuum and the dynamical origin of the symmetry breakdown is not at all understood. One of the motivations of lattice studies of the standard model is to find its limitations by analyzing its internal consistency as a quantum field theory at a non-perturbative level. More generally lattice studies aim to gain deeper understanding of the properties of coupled scalar-fermion-gauge field theories which may prove important for possible extensions of the standard model.

5.1. Upper bound on the Higgs boson mass

In the standard model the $SU(2)_L \times U(1)_Y$ gauge coupling constants are small at the electro-weak scale, and so are the Yukawa couplings of light quarks. Except for the possible of influence of a heavy top quark, one may therefore ignore the gauge bosons and fermions in the first approximation, and study the Higgs sector alone. This is an $O(4)$ invariant scalar field theory.

It is important to note that the mass formula

$$m_W = \frac{1}{2} g_2 v_r, \tag{15}$$

relating the gauge boson mass and the $SU(2)$ gauge coupling constant g_2 and the renormalized Higgs field expectation value v_r remains valid for arbitrary values of the Higgs self-coupling as long as g_2 is treated perturbatively.[12] It is this fact which allows to fix the physical scale of the Higgs sector $v_r \approx 250$GeV even if it is strongly coupled.

It has long been suspected[147] that scalar field theories in d dimensions are trivial for $d \geq 4$ in that the renormalized four-point coupling constant λ_r vanishes as the ultraviolet cutoff Λ goes to infinity irrespective of the value of the bare coupling λ_0. This was established within the lattice cutoff rigorously for $d \geq 5$[148] and semi-analytically using strong-coupling expansion and renormalization group techniques for $d = 4$.[13]

Perturbative couplings of the $SU(2)$ gauge fields around $g_2 = 0$ does not destroy the triviality.[149] Numerical simulations of lattice Higgs models including $SU(2)$ gauge fields[150] and fermions[151] further indicate that $g_2 = 0$ is the only point for the gauge coupling where a continuum limit relevant for the standard model may be taken. The standard model therefore should be an effective theory valid only up to the energy scale of an intrinsic cutoff Λ.

The triviality means that the maximum value of the renormalized Higgs coupling λ_r allowed for a given value of the cutoff Λ decreases for a larger Λ. In view of the tree-level formula

$$m_H = \sqrt{\frac{\lambda_r}{3}}v_r, \tag{16}$$

this implies the existence of an upper bound on the Higgs boson mass m_H.[11,12] A quantitative determination of the bound requires a non-perturbative evaluation of the ratio m_H/v_r since λ_r is not necessarily small for small values of Λ. For the hypercubic lattice in 4 dimensions such calculations were made a few years ago both by semi-analytical methods[13] and numerical simulations[14,15] and the upper bound was obtained.[152]

The analysis of the bound has since been refined in several respects. One of the problems of numerical simulations, already examined at some length in the previous work[14,15], is controlling finite-size effects in the broken phase due to the presence of massless Nambu-Goldstone bosons.[153,154] A recent work[155] reexamined the problem using the method of introducing a small symmetry breaking external field. Numerical data were found to be in excellent agreement with the finite-size scaling predictions worked out in [154]. The infinite volume values extracted from fits of data to the predictions confirmed the previous results.

An important question left unanswered in the previous studies is the universality of the upper bound, *i.e.*, how strongly the bound depends on the cutoff scheme.[152,156] To examine this question a detailed investigation of the bound was made on an F_4 lattice.[157] This is a lattice formed by stacking the face-centered cubic lattice in the time direction with the center of the cube shifted to the corner between two successive time slices. It has a better 4-dimensional rotation property than the hypercubic lattice, and hence is expected to be a better regularization of continuum physics. In Fig. 9 we summarize the upper bound on the ratio m_H/v_r as a function of Λ/m_H obtained on the hypercubic and F_4 lattices where the cutoff is defined as $\Lambda = 1/a$ with a the lattice spacing.

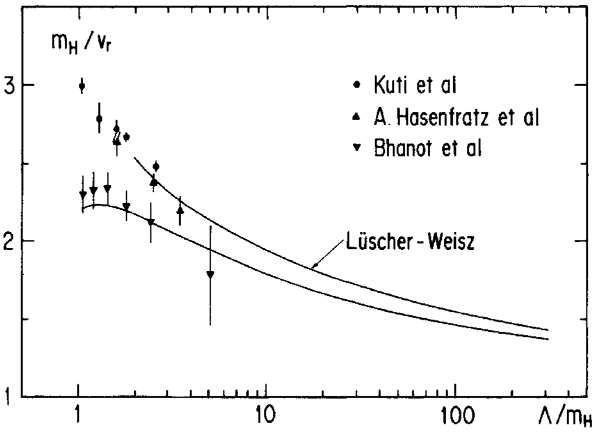

Figure 9: Upper bound on the ratio m_H/v_r ignoring gauge fields and fermions. Upper curve is the semi-analytic result[13] for the hypercubic lattice and upward triangles[14] and circles[15] simulation results. Downward triangles and lower curve are for the F_4 lattice.[157] Cutoff is defined as $\Lambda=1/a$.

The apparent difference of m_H/v_r for the two types of lattices at the same value of Λ/m_H is not physically significant since the meaning of the cutoff is different. For a proper comparison one should choose a physical criterion specifying how much cutoff-dependent effect one would allow in some physical quantity. For example[157] one may use the $90°\, W_L - W_L$ scattering cross section and demand that the deviation from the continuum value defined by

$$\delta = \frac{\frac{d\sigma^{lattice}}{d\theta}}{\frac{d\sigma^{continuum}}{d\theta}} - 1, \tag{17}$$

be less than a given fraction up to a certain center-of-mass energy E_{cm}. The upper bound obtained for this criterion with $\delta = 3\%$ or 0.3% up to $E_{cm} = 2m_W$ is listed in Table 4, together with the values for the more often used one that $\Lambda > 2m_H$. One sees that the dependence on the cutoff scheme and on the details of the criterion are both about 10%. Allowing for these uncertainties, the standard model within the $O(4)$ approximation regularized by a lattice cut-

Table 4: Upper bound on the Higgs boson mass in GeV units ignoring gauge bosons and fermions and taking v_r=250GeV. The bound for the criterion $\Lambda>2m_H$ for the hypercubic case is from [13,14,15], while that for an F_4 lattice is estimated from the data in [157]. Numbers for the criterion with δ for the F_4 lattice are from [157] correcting for a different choice of v_r (247GeV is used in [157]). For the hypercubic lattice we used data in[13,14,15] and Fig. 3 of the first paper of [157] (our estimate for the δ<0.3% case is somewhat larger than that given in [157]).

criterion	hypercubic	F_4
$\Lambda > 2m_H$	630(30)	550(30)
$\delta < 3\%$	650(30)	600(60)
$\delta < 0.3\%$	540(30)	540(60)

off cannot accomodate a Higgs boson of a mass exceeding 600(60)GeV.

This value is not much smaller than the tree-level unitarity bound $m < 800$GeV given in [13] improving the original result of [158]. The reason is that the renormalized Higgs coupling $\lambda_r \approx 3(m_H/v_r)^2$ stays small even for a cutoff as low as $\Lambda = m_H$. Establishing this fact is the essential achievement of the non-perturbative lattice analyses.

5.2. *Chiral fermions and Yukawa couplings*

Non-perturbative studies of the standard model are certainly incomplete without introduction of chiral fermions and their Yukawa couplings to the Higgs field. Possible influence of heavy fermions on the upper bound of the Higgs boson mass should be studied, and the triviality of Yukawa couplings and upper bounds on fermion masses are also important issues to be clarified. There is a well-known difficulty, however, in a lattice study of theories with chiral fermions. A naive lattice discretization of the continuum Dirac action leads to the emergence of 15 additional fermions (doublers) in the spectrum such that the number of left-handed and right-handed fermions are equal. The occurrence of doublers is a general phenomenon on a periodic lattice as long as the action has chiral symmetry.[159]

Overcoming this difficulty[160] and finding a lattice formulation of chiral fermions have been the focus of much recent work, and several promising proposals[161-164] have been made.[165] They are based on the method[35] used in QCD of adding a term of the form

$$S_W = w\sum_{x,\mu}\overline{\psi}(x)_L(2\psi(x)_R-\psi(x+\hat{\mu})_R-\psi(x-\hat{\mu})_R) +h.c. \quad (18)$$

This term gives a contribution proportional to w/a to the mass of doublers, making them infinitely heavy toward the continuum limit $a \to 0$. Since this term couples the left- and right-handed fields ψ_L and ψ_R, an application of this method to define chiral fermion theories often requires an enlargement of the field content so that each left-handed field is paired by a right-handed one. Since the pair generally carry different gauge quantum numbers (otherwise the theory will be vector-like) the Wilson term (18) by itself is not gauge invariant. Scalar fields of right quantum numbers, if they exist in the model, may be inserted between ψ_L and ψ_R appropriately to recover the invariance (Wilson-Yukawa term)[167,161,162]. An equivalent method is to average over gauge transformations of ψ_L and ψ_R in the path integral.[166]

There exists a lattice formulation of the standard model using the idea above with a minimal extension of the field content.[161,162] In this model the doublet $(\nu, e)_L$ and the singlet e_R are supplemented by a right-handed neutrino ν_R which is neutral under $SU(2)_L \times U(1)_Y$, and the Wilson-Yukawa term with the Higgs field is added to remove doublers.

Recently a nice analytic progress has been made in this model.[168] In the absence of conventional local Yukawa couplings of the form $y(\overline{\psi}(x)_L\phi(x)\psi_R(x)+h.c.)$, the action is invariant under a shift symmetry $\nu_R \to \nu_R+\epsilon$. The Ward identity of this symmetry guarantees that (i) the neutrino mass vanishes and (ii) the right-handed neutrino decouples completely in the continuum limit.

There are several other proposals for formulating lattice chiral fermion theories. In the method of mirror fermions[163] an additional fermion χ is introduced for each fermion ψ originally present in the model. The left- and right-handed components of the mirror fermion χ transform as the right- and left-handed components of ψ. The doublers of the two fermion fields are removed by the Wilson-Yukawa term, and couplings of the type $G_{\psi\chi}\overline{\psi}\chi$ are invoked to raise the mass of unobserved particles to a sufficiently high value.

Another approach[164] is to supplement each chiral field with a gauge-neutral field of opposite chirality. The Wilson term is formed generally without scalar fields. The resulting action explicitly breaks gauge invariance. The point of the proposal, however, is that counter terms may be chosen such that the gauge invariance is recovered and the additional fermions decoupled in the continuum limit.

Extensive numerical studies are being made to test these proposals in quantitative detail.[169–174] Because of the complexity of scalar-fermion theories with a number of coupling parameters, simpler systems with the staggered fermion action and gauge groups $Z(2)$ or $U(1)$ have also been studied.[175–181]

The first question in the analysis of these models is to map out the phase diagram in the space of Higgs and Yukawa couplings and find second order phase transitions where a continuum limit may exist. The phase diagram turned out to be quite complex[179,180,181,171], being divided into a number of phases with distinct behaviors of the Higgs field expectation value v and that of the fermion mass. The effect of fermions is strong for intermediate values of the Yukawa coupling, enlarging the broken phase with $v \neq 0$. As a result the symmetric phase with $v = 0$ is generally split into two parts, one for small Yukawa coupling y and the other for large y. The boundary between the broken phase and the symmetric phase for large y has the distinctive characteristic that the fermion mass increases as the Higgs expectation value decreases toward the boundary[178,170,172,165], contrary to the perturbative behavior $m_f \propto y \cdot v$ for small y.

Boundary lines separating symmetric and broken phases appear to be generally of second order, allowing a continuum limit to be taken. For the limit to be meaningful, the mass of physical fermions has to stay finite while that of doublers should become large as $\mathcal{O}(1/a)$ as the lattice spacing $a \to 0$. We expect that the latter requires a large Wilson-Yukawa coupling. In fact for small w the doubler mass is proportional to $w \cdot v$ which does not diverge as $a \to 0$ since v remains finite. Recent results for several models give evidence that the doubler mass remains $\mathcal{O}(1/a)$ as the phase transition point is approached if the Wilson-Yukawa coupling is sufficiently large.[169,170,172,173]

5.3. *Strong-coupling QED*

The triviality of QED is a long-standing problem of quantum field theory. This problem has received renewed interest from the observation[182] that the ladder approximation to the Schwinger-Dyson equation gives an ultraviolet fixed point with a non-trivial scaling property. Above the fixed point chiral symmetry is spontaneously broken. An interacting theory may exist around the fixed point, which, if valid, may have implications for models of the electro-weak symmetry breaking mechanism.

The question has been investigated both in the continuum (see [183–185] for some recent work) and on a lattice.[16,186–193] Numerical simulations have confirmed the existence of a phase transition separating the weak-coupling phase from a strong-coupling phase with spontaneously broken chiral symmetry. The phase transition, however, is of first-order for the usual Wilson gauge action[186], except possibly at the end-point of the first-order line.[187] The continuum limit is difficult to construct for this form of lattice QED.

The phase transition is of second order for the non-compact action obtained by a straightforward discretization of the continuum one.[16,189,190,192] For the case of 4 fermion flavors, however, the recent studies[183,185,190–193], especially the numerical result[192] that the Callan-Symanzik β function for the renormalized charge stays positive across the critical point and smoothly matches on to the 1-loop perturbative formula, support that the continuum limit defined at the critical point is a non-interacting theory, contrary to an earlier claim.[16,189] The question is not settled yet for smaller number of flavors[189] including the case of the quenched approximation.[188,192]

6. Conclusion and outlook

There has been much development in lattice field theories since the last High Energy Conference at Munich. The main points may be summarized as follows:

- The nucleon to ρ mass ratio decreases and becomes closer to the experimental value 1.22 as the lattice spacing a is reduced. In the quenched approximation which ignores sea quarks the recent simulations give $m_N/m_\rho \sim 1.3$ at $a \sim 0.1$fm. Serious effort is being made to improve the hadron spectrum calculation including sea quarks.

- The calculation of weak matrix elements has been pushed ahead with large scale quenched simulations using the techniques previously developed. The latest results for the K meson B parameter suggest the presence of a sizable finite lattice spacing correction. The method of effective action for heavy quarks has been tested, giving unexpectedly large values for the B meson decay constant. The $K \to \pi\pi$ processes are still not understood well.

- The deconfining phase transition of the pure $SU(3)$ gauge theory at finite temperatures is of first order in agreement with the theoretical prediction. The previous controversy on this question has been fully resolved.

- The finite-temperature chiral phase transition in the presence of light quarks is also of first order if the number of flavors is four. For the case of two flavors, on the other hand, a phase transition appears absent down to the quark mass $m_q/T \sim 0.05$.

- The upper bound on the Higgs boson mass with a lattice cutoff may be summarized as $m_H < 600(60)$GeV within the approximation of treating the gauge bosons and fermions perturbatively. The uncertainty arises from the dependence of the bound on the lattice structure and the criterion on the magnitude of cutoff effects, which is estimated from the results of studies on a hypercubic and an F_4 lattice.

- Extensive work is being made of Higgs-chiral fermion systems. The phase diagram of a number of models have been studied to locate second-order phase transitions where a continuum limit may be taken. In a class of models decoupling of extra fermions introduced for the consistency of the model is guaranteed for a large cutoff by an exact symmetry without tuning of parameters. Numerical simulations support that doublers also decouple for a sufficiently large Wilson-Yukawa coupling.

- Evidence is accumulating that the continuum limit of non-compact lattice QED is trivial for four fermion flavors.

The lattice formulation and computer simulations provide a powerful method for analyzing non-perturbative phenomena in quantum field theories. Over the years it has progressed into one of our basic tools for extracting quantitative predictions of realistic field theories, and a number of results have been obtained over a wide range of problems in particle physics. It should be clear, however, that further improvement of results are needed in many of the problems. An important ingredient for this purpose is a substantial increase of the computing power. This need is particularly acute in lattice QCD. Indeed full QCD simulations with realistically light quarks and a small lattice spacing on a correspondingly larger lattice (*e.g.*, $m_q \sim 5$MeV, $a \sim 0.1-0.05$fm and 48^4) involves an amount of computations at least a factor $\mathcal{O}(10^3)$ greater than the ones made today. Since computers presently available have the typical speed of a few Gigaflops (1 Gigaflop=10^9 arithmetic operations per second) this puts the necessary speed in the range of Teraflops.

In order to see the prospect toward such a speed we plot in Fig. 10 the progress of computers since 1979 when lattice field theory simulations began. The open symbols are for commercial supercomputers and the solid ones for special-purpose computers built by physicists. Four hand-made computers, three at Columbia and one by the APE Collaboration in Rome, have been in operation, producing physics results in lattice QCD, and the construction of several other computers (GF11 at IBM[22], QCD-PAX at Tsukuba[24] and ACPMAPS at FNAL[25]) are nearly completed. It is interesting to note that the speed of dedicated computers have been increasing 10-fold every 2-3 years, which is roughly double that of commercial supercomputers. Further along the line of development is the APE100 project by the Rome group[194] which is well underway, and a collaboration in the United States have recently proposed the construction of a Teraflop computer.[195]

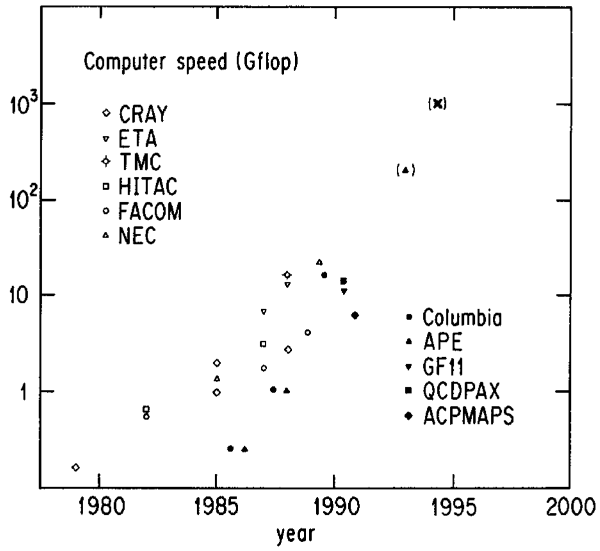

Figure 10: Progress of computer speed with years. Open symbols are for commercial supercomputers and filled ones for special purpose computers for lattice simulations. The symbol second from right marks the target of the APE100 project[194], and the right-most symbol represent the goal of the recent proposal for a Teraflop computer.[195]

Lattice field theory simulations have the merit that results could be systematically improved by reducing the lattice spacing, enlarging the lattice size and increasing statistics, without recourse to approximations. Progress in lattice field theory will continue as this merit will become utilized more fully with the coming of more powerful computers.

Acknowledgements

I would like to thank Norman Christ, Elbio Dagotto, Masataka Fukugita, Steven Gottlieb, Rajan Gupta, Urs Heller, Yoichi Iwasaki, Kazuyuki Kanaya, Enzo Marinari, Guido Martinelli, Masanori Okawa, Robert Schrock, Amarjit Soni, Michael Teper and Thomas Walsh for discussion and correspondence while preparing and writing this review.

REFERENCES

1. K. G. Wilson, Phys. Rev. **D10** (1974) 2445.
2. M. Creutz, L. Jacobs and C. Rebbi, Phys. Rev. Lett. **42** (1979) 1390.
3. M. Creutz, Phys. Rev. Lett. **43** (1979) 553 ; Phys. Rev. **D21** (1980)2308; Phys. Rev. Lett. **45** (1980) 313.
4. H. Hamber and G. Parisi, Phys. Rev. Lett. **47** (1981) 1792; E. Marinari, G. Parisi and C. Rebbi, Phys. Rev. Lett. **47** (1981) 1795.
5. D. Weingarten, Phys. Lett. **109B** (1982) 57.
6. R. Hagedorn, Nuovo Cim. Supp. **3** (1965) 147; N. Cabibbo and G. Parisi, Phys. Lett. **59B** (1975) 67.
7. A. M. Polyakov, Phys. Lett. **72B** (1978) 477; L. Susskind, Phys. Rev. **D20** (1979) 2610.
8. N. Cabibbo, G. Martinelli and R. Petronzio, Nucl. Phys. **B244** (1984) 381.
9. R. C. Brower, G. Maturana, M. B. Gavela and R. Gupta, Phys. Rev. Lett. **53** (1984) 1318.
10. C. Bernard, T. Draper, G. Hockney, A. M. Rushton and A. Soni, Phys. Rev. Lett. **55** (1985) 2770.
11. L. Maiani, G. Parisi and R. Petronzio, Nucl. Phys. **B136** (1978) 115.
12. R. Dashen and H. Neuberger, Phys. Rev. Lett. **50** (1983) 1897.
13. M. Lüscher and P. Weisz, Nucl. Phys. **B290**[FS20] (1987) 25; **B295**[FS21] (1988) 65; **B318** (1989) 705; Phys. Lett. **B212** (1989) 472.
14. A. Hasenfratz, K. Jansen, C. B. Lang, T. Neuhaus and H. Yoneyama, Phys. Lett. **B199** (1987) 531; A. Hasenfratz, K. Jansen, J. Jersák, C. B. Lang, T. Neuhaus and H. Yoneyama, Nucl. Phys. **B317** (1989) 81; T. Neuhaus, in *Lattice 88*, Nucl. Phys. **B**(Proc. Suppl.) **9** (1989) 21.
15. J. Kuti, L. Lin and Y. Shen, Phys. Rev. Lett. **61** (1988) 678; in *Lattice 87*, Nucl. Phys. **B**(Proc. Suppl.) **4** (1988) 397;in *Lattice 88*, Nucl. Phys. **B**(Proc. Suppl.) **9** (1989) 26.
16. J. B. Kogut, E. Dagotto and A.Kocić, Phys. Rev. Lett. **60** (1988) 772.
17. See, *e.g.*, J. Ambjørn, T. Askgaard, H. Porter and M. E. Shaposhnikov, Phys. Lett. **B244** (1990) 479; D. Yu. Grigoriev, V. A. Rubakov and M. E. Shaposhnikov, Nucl. Phys. **B326** (1989) 737.
18. For a review, see F. David, in *Lattice 89*, Nucl. Phys. **B**(Proc. Suppl.) **17** (1990) 51.
19. For a review, see D. Weingarten, in *Lattice 88*, Nucl. Phys. **B**(Proc. Suppl.) **9** (1989) 447.
20. E. Brooks, III, G. Gox, M. Johnson, S. Otto, P. Stolorz, W. Athnas, E. DeBenedictis, R. Faucette. C. Seitz and J. Stack, Phys. Rev. Lett. **52** (1984) 2324.

21. N. H. Christ and A. E. Terrano, IEEE Trans. Comp. **33** (1984) 344; N. H. Christ, in *Lattice 89*, Nucl. Phys. **B**(Proc. Suppl.) **17** (1990) 267.

22. J. Beetem, M. Denneau and D. Weingarten. in *The 12th Annual International Symposium on Computer Architecture*, (IEEE Computer Society Press, Silver Spring, Maryland, 1985) 108; D. Weingarten, in *Lattice 89*, Nucl. Phys. **B**(Proc. Suppl.) **17** (1990) 272.

23. P. Bacilieri *et al.*, in *Computing in High Energy Physics* (Amsterdam, 1985), ed. L. O. Hertzberger and W. Hoogland (North Holland, Amsterdam, 1986) 330.

24. Y. Iwasaki, T. Hoshino, T. Shirakawa, Y. Oyanagi and T. Kawai, Comp. Phys. Comm. **49** (1988) 449; Y. Oyanagi, contribution to the parallel session (paper #549).

25. P. Mackenzie, E. Eichten, G. Hockney, H. B. Thacker, R. Atac, A. Cook, M. Fischler, I. Gaines, D. Husby and T. Nash, in *Lattice 87*, Nucl. Phys. **B**(Proc. Suppl.) **4** (1988) 580.

26. A. Ukawa, Nucl. Phys. **B**(Proc. Suppl.)**10A** (1989) 66.

27. E. Marinari, in *Lattice 88*, Nucl. Phys. **B**(Proc. Suppl.) **9** (1989) 209.

28. The APE Collaboration, P. Bacilieri, E. Remiddi, G. M. Tedesco, S. Cabasino, N. Cabibbo, E. Marinari, P. Paolucci, G. Parisi, J. Pech, G. Salina, M. P. Lombardo, R. Tripiccione, F. Marzano, F. Rapuano, R. Sarno and W. Tross, Nucl. Phys. **B343** (1990) 228; S. Cabasino *et al.*, in *Lattice 89*, Nucl. Phys. **B**(Proc. Suppl.) **17** (1990) 431; E. Marinari, private communication.

29. T. Yoshié, Y. Iwasaki and S. Sakai, in *Lattice 89*, Nucl. Phys. **B**(Proc. Suppl.) **17** (1990) 413.

30. R. Gupta, G. Guralnik, G. W. Kilcup and S. R. Sharpe, preprint LAUR-90-3050 (1990); R. Gupta, in *Lattice 89*, Nucl. Phys. **B**(Proc. Suppl.) **17** (1990) 70.

31. The APE Collaboration, presented by M. Guagnelli at *Lattice 90*, Tallahassee, Florida (October 8-12, 1990) .

32. A. Billoire, E. Marinari and G. Parisi, Phys. Lett. **162B** (1985) 160; The APE Collaboration, P. Bacilieri *et al.*, Nucl. Phys. **B317** (1989) 509.
See also S. Güsken, U. Löw, K.-H. Mütter, R. Sommer, A. Patel and K. Schilling, in *Lattice 89*, Nucl. Phys. **B**(Proc. Suppl.) **17** (1990) 361.

33. S. Ono, Phys. Rev. D**17** (1978) 888.

34. M. Fukugita, Y. Oyanagi and A. Ukawa, Phys. Rev. D**36** (1987) 824.

35. K. G. Wilson, in *New Phenomena in Subnuclear Physics*, ed. A. Zichichi (Plenum, New York, 1977) 69.

36. H. Kluberg-Stern, A. Morel and B. Petersson, Nucl. Phys. **B215**[FS7] (1983) 527.

37. S. Gottlieb, W. Liu, R. L. Renken, R. L. Sugar and D. Toussaint, Phys. Rev. D**38** (1988) 2245.

38. The APE Collaboration, P. Bacilieri *et al.*, Phys. Lett. **B205** (1988) 535.

39. C. Michael and M. Teper, Nucl. Phys. **B314** (1989) 347.

40. G. Schierholz, in *Lattice 88*, Nucl. Phys. **B**(Proc. Suppl.) **9** (1989) 244.

41. A. D. Kennedy, J. Kuti, S. Meyer and B. Pendleton, Phys. Rev. Lett. **54** (1985) 87; S. Gottlieb, J. Kuti, D. Toussaint, A. D. Kennedy, S. Meyer, D. J. Pendleton and R. L. Sugar, Phys. Rev. Lett. **55** (1985) 1958.

42. N. H. Christ, in *Lattice 89*, Nucl. Phys. **B**(Proc. Suppl.) **17** (1990) 267.

43. For a recent study of these quantities using the cooling method, see A. Di Giacomo, contribution to the parallel session (paper #129-132).

44. The High Energy Monte Carlo Grand Challenge Collaboration, K. M. Bitar, R. Edwards, U. M. Heller, A. D. Kennedy, W. Liu, T. A. DeGrand, S. Gottlieb, A. Krasnitz, J. B. Kogut, R. L. Renken, M. C. Ogilvie, P. Rossi, D. K. Sinclair, K. C. Wang, R. L. Sugar, M. Teper and D. Toussaint, Phys. Rev. Lett. **65** (1990) 2106; preprint FSU-SCRI-90-98 (1990). See also K. M. Bitar *et al.*, in *Lattice 89*, Nucl. Phys. **B**(Proc. Suppl.) **17** (1990) , 400,404.

45. A. Patel, R. Gupta, G. W. Kilcup and S. R. Sharpe, Phys. Lett. **B225** (1989) 398; A. Patel, in *Lattice 89*, Nucl. Phys. **B**(Proc. Suppl.) **17** (1990) 509; C. Baillie, R. Brickner, R. Gupta, G. W. Kilcup, A. Patel and S. R. Sharpe, in progress (reported by R. Gupta at *Lattice 90*, Tallahassee, Florida (October 8-12, 1990)).

46. F. R. Brown, F. P. Butler, H. Cheng, N. H. Christ, Z. Dong, W. Schaffer, L. I. Unger and A. Vaccarino, in progress (reported by H. Cheng at *Lattice 90*, Tallahassee, Florida (October 8-12, 1990)).

47. M. Fukugita, H. Mino, M. Okawa and A. Ukawa, in progress (reported by A. Ukawa at *Lattice 90*, Tallahassee, Florida (October 8-12, 1990)).

48. The MT$_c$ Collaboration, R. Altmeyer, K. D. Born, W. S. Ibes, E. Laermann, T. F. Walsh and P. M. Zerwas, presented by T. F. Walsh at the

parallel session (paper #604 (preprint UMN-TH-838/90 (1990))). See also E. Laermann *et al.*, in *Lattice 89*, Nucl. Phys. **B**(Proc. Suppl.) **17** (1990) 436.

49. S. Itoh, Y. Iwasaki and T. Yoshié, Phys. Lett. **B184** (1987) 375; Phys. Rev. D**36** (1987) 527. See also [34] and M. Fukugita, T. Kaneko and A. Ukawa, Phys. Lett. **145B** (1984) 93.
50. J. Gasser, H. Leutwyler and M. E. Sainio, preprint BUTP-90/30 (1990).
51. L. Maiani, G. Martinelli, M. Paciello and B. Taglienti, Nucl. Phys. **B293** (1987) 420.
52. S. Güsken, K. Schilling, R. Sommer, K.-H. Mütter and A. Patel, Phys. Lett. **B212** (1988) 216.
53. For a preliminary attempt, see A. Patel, [45].
54. The EMC Collaboration, Nucl. Phys. **B328** (1989) 1. For the recent experimental status, see the plenary talk of F. Close, in these proceedings.
55. J. Ellis, R. Flores and S. Ritz, Phys. Lett. **B198** (1987) 393.
56. G. Altarelli and G. G. Ross, Phys. Lett. **B212** (1988) 391;
R. D. Carlitz, J. C. Collins and A. H. Mueller, Phys. Lett. **B214** (1988) 229.
57. J. E. Mandula, contribution to the parallel session (paper #432).
58. S. Güsken, U. Löw, K.-H. Mütter, R. Sommer, A. Patel and K.Schilling, Phys. Lett. **B227** (1989) 266; in *Lattice 89*, Nucl. Phys. **B**(Proc. Suppl.) **17** (1990) 513.
59. S. Aoki and A. Gocksch, Phys. Rev. Lett. **63** (1989) 1125.
60. S. Aoki, A. Gocksch, A. V. Manohar and S. R. Sharpe, Phys. Rev. Lett. **65** (1990) 1092.
61. W. Wilcox and R. M. Woloshyn, Phys. Rev. Lett. **54** (1985) 2653; T. Draper, R. M. Woloshyn, W. Wilcox and K.-F. Liu, Nucl. Phys. **B318** (1989) 319.
62. G. Martinelli and C. T. Sachrajda, Nucl. Phys. **B306** (1988) 865.
63. G. Martinelli and C. T. Sachrajda, Nucl. Phys. **B316** (1989) 355.
64. G. Martinelli, in *Lattice 88*, Nucl. Phys. **B**(Proc. Suppl.) **9** (1989) 134.
65. T. Draper, R. M. Woloshyn and K.-F. Liu, Phys. Lett. **B234** (1990) 121; W. Wilcox, K.-F. Liu, T. Draper and C. M. Wu, in *Lattice 89*, Nucl. Phys. **B**(Proc. Suppl.) **17** (1990) 382; K.-F .Liu, contribution to the parallel session (paper #148).
66. M. Lüscher, Nucl. Phys. **B219** (1983) 233.
67. J. Koller and P. van Baal, Phys. Rev. Lett. **58** (1987) 2511; Nucl. Phys. **B302** (1988) 1.
68. C. Vohwinkel, Phys. Rev. Lett. **63** (1989) 2544.
69. P. van Baal, Phys. Lett. **B224** (1989) 397.
70. P. van Baal and A. S. Kronfeld, in *Lattice 88*, Nucl. Phys. **B**(Proc. Suppl.) **9** (1989) 227.
71. The High Energy Monte Carlo Grand Challenge Collaboration, private communication from M. Teper.
72. R. L. Jaffe, Phys. Rev. Lett. **38** (1977) 195.
73. Y. G. Liang, B. A. Li, K.-F. Liu, T. Draper and R. M. Woloshyn, in *Lattice 89*, Nucl. Phys. **B**(Proc. Suppl.) **17** (1990) 408; K.-F .Liu, contribution to parallel session (paper #148).
74. C. Bernard and A. Soni, in *Lattice 88*, Nucl. Phys. **B**(Proc. Suppl.) **9** (1989) 155.
75. E. Eichten, G. Hockney and H. B. Thacker, in *Lattice 89*, Nucl. Phys. **B**(Proc. Suppl.) **17** (1990) 529.
76. C. R. Allton, C. T. Sachrajda, V. Lubicz, L. Maiani and G. Martinelli, preprint Shep89/90-11(1990); Ph. Boucaud, O. Pene, V. J. Hill, C. T. Sachrajda and G. Martinelli, Phys. Lett. **B220** (1989) 219.
77. C. Alexandrou, F. Jegerlehner, S. Güsken, K. Schilling and R. Sommer, preprint WU-B-90 (1990).
78. A. Soni, contribution to the parallel session; J. Labrenz, talk at *Lattice 90*, Tallahassee, Florida (October 8-12, 1990) .
79. E. Eichten, in *Lattice 87*, Nucl. Phys. **B**(Proc. Suppl.) **4** (1988) 170.
80. T. A. DeGrand and R. D. Loft, Phys. Rev. D**38** (1988) 954.
81. M. B. Gavela, L. Maiani, S. Petrarca, F. Rapuano, G. Martinelli, O. Pene and C. T. Sachrajda, Nucl. Phys. **B306** (1988) 677.
82. M. B. Gavela, L. Maiani, S. Petrarca, G. Martinelli and O. Pene, Phys. Lett. **B206** (1988) 113.
83. C. Bernard, T. Draper, G. Hockney and A. Soni, Phys. Rev. D**38** (1988) 3540.
84. Ph. Boucaud, C. L. Lin and O. Pene, Phys. Rev. D**40** (1989) 1529.
85. E. Eichten abd B. Hill, Phys. Lett. **B234** (1989) 511; **B240** (1990) 193; **B243** (1990) 427.

86. C. Bernard, A. El-Khadra and A. Soni, in *Lattice 89*, Nucl. Phys. **B**(Proc. Suppl.) **17** (1990) 499.

87. M. Crisafulli, G. Martinelli, V. J. Hill and C. T. Sachrajda, Phys. Lett. **B223** (1989) 90.

88. V. Lubicz, G. Martinelli and C. T. Sachrajda, Rome preprint (1990).

89. The Tagged Photon Spectrometer Collaboration, J. C. Anjos *et al.*, Phys. Rev. Lett. **62** (1989) 1587; The Mark III Collaboration, J. Adler *et al.*, Phys. Rev. Lett. **62** (1989) 1821.

90. The Tagged Photon Spectrometer Collaboration, presented by B. Reay(E653) at the parallel session; preprint UCSB-HEP-90-11 (1990).

91. See, for example, M. Wirbel, B. Stech and M. Bauer, Z. Phys. **C29** (1985) 637; B. Grinstein and M. Wise, Phys. Lett. **B197** (1987) 249; D. Scora and N. Isgur, Phys. Rev. **D40** (1989) 1491.

92. G. Martinelli, in *Lattice 89*, Nucl. Phys. **B**(Proc. Suppl.) **17** (1990) 523. See also [81].

93. C. Bernard and A. Soni, in *Lattice 89*, Nucl. Phys. **B**(Proc. Suppl.) **17** (1990) 495.

94. G. W. Kilcup, S. R. Sharpe, R. Gupta and A. Patel, Phys. Rev. Lett. **64** (1990) 25.

95. S. R. Sharpe, talk at *Lattice 90*, Tallahassee, Florida (October 8-12, 1990) .

96. G. W. Kilcup and S. R. Sharpe, Nucl. Phys. **B283** (1987) 493.

97. J. F. Donoghue, E. Golowich and B. R. Holstein, Phys. Lett. **119B** (1982) 412.

98. A. Pich and E. DeRafael, Phys. Lett. **158B** (1985) 477.

99. R. Decker, Nucl. Phys. **B**(Proc. Suppl.)**7A** (1989) 180.

100. W. A. Bardeen, A. J. Buras and J.-M. Gérard, Phys. Lett. **B211** (1988) 343.

101. C. Bernard, T. Draper, G. Hockney and A. Soni, in *Lattice 87*, Nucl. Phys. **B**(Proc. Suppl.) **4** (1988) 483.

102. M. B. Gavela, L. Maiani, S. Petrarca, G. Martinelli and O. Pene, Phys. Lett. **B211** (1988) 139.

103. G. W. Kilcup, in *Lattice 89*, Nucl. Phys. **B**(Proc. Suppl.) **17** (1990) 533; R. Gupta, private communication.

104. S. R. Sharpe, R. Gupta, G. Guralnik, G. W. Kilcup and A. Patel, Phys. Lett. **B192** (1987) 149.

105. E. Franco, L. Maiani, G. Martinelli and A. Morelli, Nucl. Phys. **B317** (1989) 63.

106. C. Bernard, J. Simone and A. Soni, in *Lattice 89*, Nucl. Phys. **B**(Proc. Suppl.) **17** (1990) 504.

107. The European Lattice Collaboration, A. Abada, Ph. Boucaud, M. Crisafulli, E. Franco, M. B. Gavela, V. J. Hill, G. Martinelli, O. Pene and C. T. Sachrajda, in *Lattice 89*, Nucl. Phys. **B**(Proc. Suppl.) **17** (1990) 518.

108. L. Maiani, G. Martinelli, G. C. Rossi and M. Testa, Nucl. Phys. **B289** (1987) 505.

109. C. Bernard, T. Draper, A. Soni, H. D. Politzer and M. B. Wise, Phys. Rev. D**32** (1985) 2343.

110. S. R. Sharpe, in *Lattice 89*, Nucl. Phys. **B**(Proc. Suppl.) **17** (1990) 146.

111. M. Lüscher, Commun. Math. Phys. **104** (1986) 177; **105** (1986) 153.

112. M. Guagnelli, E. Marinari and G. Parisi, Phys. Lett. **B240** (1990) 188.

113. L. D. McLerran and B. Svetitsky, Phys. Lett. **98B** (1981) 195; J. Kuti, J. Polónyi and K. Szlachányi, Phys. Lett. **98B** (1981) 199.

114. K. Kajantie, C. Montonen and E. Pietarinen, Z. Phys. **C9** (1981) 253;
J. B. Kogut, M. Stone, H. W. Wyld, W. R. Gibbs, J. Shigemitsu, S. H. Shenker and D. K. Sinclair, Phys. Rev. Lett. **50** (1983) 393;
T. Çelik, J. Engels and H. Satz, Phys. Lett. **125B** (1983) 411.

115. See the reviews, M. Fukugita, in *Lattice Gauge Theory using Parallel Processors*, ed. X. Y. Li, Z. M. Qiu and H. C. Ren, (Gordon and Breach, London, 1987) 195; A. Ukawa, [26].

116. B. Svetitsky and L. G. Yaffe, Nucl. Phys. **B210**[FS6] (1982) 423.

117. T. Banks and A. Ukawa, Nucl. Phys. **B225**[FS9] (1983) 145; T. A. DeGrand and C. E. DeTar, Nucl. Phys. **B225**[FS9] (1983) 590.

118. R. D. Pisarski and F. Wilczek, Phys. Rev. D29 (1984) 338.

119. The APE Collaboration, P. Bacilieri *et al.*, Phys. Rev. Lett. **61** (1988) 1545; Nucl. Phys. **B318** (1989) 553; Phys. Lett. **B220** (1989) 607; Phys. Lett. **B224** (1989) 333.

120. F. R. Brown, N. H. Christ, Y. Deng, M. Gao and T. J. Woch, Phys. Rev. Lett. **61** (1988) 2058.

121. M. Fukugita, M. Okawa and A. Ukawa, Phys. Rev. Lett. **63** (1989) 1768; Nucl. Phys. **B337** (1990) 181.

122. For a detailed account of all aspects of the problem, see A. Ukawa, in *Lattice 89*, Nucl. Phys. **B**(Proc. Suppl.) **17** (1990) 118.

123. See, *e.g.,* M. N. Barber in *Phase transitions and critical phenomena*, Vol. 8, eds. C. Domb and J. Lebowitz (Academic Press, New York, 1983) 145.

124. The APE Collaboration, S. Cabasino *et al.*, in *Lattice 89*, Nucl. Phys. **B**(Proc. Suppl.) **17** (1990) 218.

125. I. R. McDonald and K. Singer, Discuss. Faraday Soc. **43** (1967) 40; A. M. Ferrenberg and R. H. Swendsen, Phys. Rev. Lett. **61** (1988) 2635; Phys. Rev. Lett. **63** (1989) 1195.

126. F. R. Brown and N. H. Christ, cited in [122].

127. R. V. Gavai, F. Karsch and B. Petersson, Nucl. Phys. **B322** (1989) 738; S. Gupta, A. Irbäck, B. Petersson, R. V. Gavai and F. Karsch, Nucl. Phys. **B329** (1990) 263.

128. M. Fukugita, H. Mino, M. Okawa and A. Ukawa, J. Stat. Phys. **59** (1990) 1397; M. Fukugita and M. Okawa, Phys. Rev. Lett. **63** (1989) 13.

129. A. Billoire, R. Lacaze and A. Morel, in *Lattice 89*, Nucl. Phys. **B**(Proc. Suppl.) **17** (1990) 230.

130. R. V. Gavai and F. Karsch, Phys. Lett. **B233** (1989)417.

131. S. Gottlieb, W. Liu, R. L. Renken, R. L. Sugar and D. Toussaint, Phys. Rev. D40 (1989) 2389.

132. The MT_c Collaboration, R. V. Gavai, S. Gupta, A. Irbäck, F. Karsch, S. Meyer,B. Petersson, H. Satz and H. W. Wyld, Phys. Lett. **B232** (1989) 491; Phys. Lett. **B241** (1990) 567; B. Petersson, contribution to the parallel session (paper #418).

133. M. Fukugita, H. Mino, M. Okawa and A. Ukawa, Phys. Rev. Lett. **65** (1990) 816; Phys. Rev. D**42** (1990) 2936.

134. F. R. Brown, F. P. Butler, H. Cheng, N. H. Christ, Z. Dong, W. Schaffer, L. I. Unger and A. Vaccarino, Phys. Rev. Lett. **65** (1990) 2491; A. Vaccarino, talk at *Lattice 90*, Tallahassee, Florida (October 8-12, 1990) .

135. F. R. Brown, F. P. Butler, H. Cheng, N. H. Christ, Z. Dong, W. Schaffer, L. I. Unger and A. Vaccarino, preprint CU-TP-474.

136. J. B. Kogut and D. K. Sinclair, preprint Ill-(TH)-90-#7 (1990).

137. For a recent work, see, K. P. Enqvist, contribution to the parallel session (paper #164,165).

138. K. Kajantie, L. Kärkkäinen and K. Rummukainen, Nucl. Phys. **B333** (1990) 100.

139. J. Potvin and C. Rebbi, in *Lattice 89*, Nucl. Phys. **B**(Proc. Suppl.) **17** (1990) 223.

140. F. Karsch, in *Lattice 88*, Nucl. Phys. **B**(Proc. Suppl.) **9** (1989) 357;
B. Petersson, in *Quark Matter 90* (BU-TP90/28(1990)).

141. I. Barbour, N. E. Bihilil, E. Dagotto, F. Karsch, A. Moreo, M. Stone and H. W. Wyld, Nucl. Phys. **B275**[FS17] (1986) 296.

142. P. E. Gibbs, Phys. Lett. **B182** (1986) 369.

143. D. Toussaint, in *Lattice 89*, Nucl. Phys. **B**(Proc. Suppl.) **17** (1990) 248.

144. E. Dagotto, A. Moreo and U. Wolff, Phys. Rev. Lett. **57** (1986) 1292; Phys. Lett. **B186** (1987) 395;
F. Karsch and K.-H. Mütter, Nucl. Phys. **B313** (1989) 541.

145. A. Gocksch, Phys. Rev. Lett. **61** (1988) 2054.

146. I. M. Barbour, C. T. H. Davies and Z. Sabeur, Phys. Lett. **B215** (1988) 567; I. M. Barbour, in *Lattice 89*, Nucl. Phys. **B**(Proc. Suppl.) **17** (1990) 243.

147. K. G. Wilson and J. B. Kogut, Phys. Rep. **12** (1974) 75.

148. M. Aizenmann, Phys. Rev. Lett. **47** (1981) 1; J. Fröhlich, Nucl. Phys. **B200**[FS4] (1982) 281.

149. A. Hasenfratz and P. Hasenfratz, Phys. Rev. **D34** (1986) 3160.

150. W. Bock, H. G. Evertz, J. Jersák, D. P. Landau, T. Neuhaus and J. L. Xu, Phys. Rev. **D41** (1990) 2573 and references cited therin.

151. S. Meyer and B. Pendleton, preprint Edinburgh 90/481 (1990) and references cited therein.

152. For reviews, see, P. Hasenfratz, in *Lattice 88*, Nucl. Phys. **B**(Proc. Suppl.) **9** (1989) 3;
H. Neuberger, in *Lattice 89*, Nucl. Phys. **B**(Proc. Suppl.) **17** (1990) 17.

153. H. Neuberger, Phys. Rev. Lett. **60** (1988) 889; Nucl. Phys. **B300**[FS22] (1988) 180.

154. P. Hasenfratz and H. Leutwyler, Nucl. Phys. **B343** (1990) 241 and references cited therein.

155. A. Hasenfratz, K. Jansen, J. Jersák, C. B. Lang, H.Leutwyler and T. Neuhaus, Z. Phys. **C46** (1990) 257.

156. For a previous attempt, see G. Bhanot and K. M. Bitar, Phys. Rev. Lett. **61** (1988) 798; G. Bahnot, in *Lattice 88*, Nucl. Phys. **B**(Proc. Suppl.) **9** (1989) 18.

157. G. Bhanot, K. M. Bitar, U. M. Heller and H. Neuberger, Nucl. Phys. **B343** (1990) 467; preprint 90-111 (1990).

158. B. W. Lee, C. Quigg, and H. B. Thacker, Phys. Rev. D**16** (1977) 1519.

159. H. B. Nielsen and M. Ninomiya, Nucl. Phys. **B185** (1981) 20; L. H. Karsten and J. Smit, Nucl. Phys. **B183** (1981) 103.

160. For a recent work using a random lattice, see T. -W. Chiu, contribution to the parallel session (paper #66-68).

161. J. Smit, Nucl. Phys. **B175** (1980) 307; Acta Physica Polonica **B17** (1986) 531.

162. P. D. V. Swift, Phys. Lett. **145B** (1984) 256.

163. I. Montvay, Phys. Lett. **B199** (1987) 89; in *Lattice 87*, Nucl. Phys. **B**(Proc. Suppl.) **4** (1988) 443.

164. A. Borelli, L. Maiani, G. C. Rossi, R. Sisto and M. Testa, Phys. Lett. **B221** (1989) 360; Nucl. Phys. **B333** (1990) 335.

165. For a detailed review, see, J. Smit, in *Lattice 89*, Nucl. Phys. **B**(Proc. Suppl.) **17** (1990) 3.

166. S. Aoki, Phys. Rev. Lett. **60** (1988) 2109;
K. Funakubo and T. Kashiwa, Phys. Rev. Lett. **60** (1988) 2113;
T. D. Kiu, D. Sen, S.-S. Xue, Phys. Rev. Lett. **61** (1988) 282.

167. L. H. Karsten, in *Field Theoretical Methods in Particle Physics*, ed. W. Rühl (Plenum, New York, 1980) 235.

168. M. F. L. Golterman and D. N. Petcher, Phys. Lett. **B225** (1989) 159; in *Lattice 89*, Nucl. Phys. **B**(Proc. Suppl.) **17** (1990) 470, 475; preprint UCLA/90/TEP/19 (1990).

169. A. M. Thornton, Phys. Lett. **B221** (1989) 151; **B227** (1989) 434.

170. W. Bock, A. K. De, K. Jansen, J. Jersák and T. Neuhaus, Phys. Lett. **B231** (1989) 283; W. Bock, A. K. De, K. Jansen, J. Jersák, T. Neuhaus and J. Smit, Phys. Lett. **B232** (1989) 486.

171. W. Bock, A. K. De, K. Jansen, J. Jersák, T. Neuhaus and J. Smit, Nucl. Phys. **B344** (1990) 207.

172. W. Bock and A. K. De, Phys. Lett. **B245** (1990) 207.

173. S. Aoki, I.-H. Lee, J. Shigemitsu and R. E. Shrock, Phys. Lett. **B243** (1990) 403.

174. K. Farakos, G. Koutsoumbas, L. Lin, J. P. Ma, I. Montvay and G. Münster, preprint DESY 90-035 (contributed paper #285).

175. J. Shigemitsu, Phys. Lett. **B189** (1987) 164 ; Phys. Lett. **B226** (1989) 364; J. Polonyi and J. Shigemitsu, Phys. Rev. D**38** (1988) 3231.

176. D. Stephenson and A. M. Thornton, Phys. Lett. **B212** (1988) 479; A. M. Thornton, Phys. Lett. **B214** (1988) 577.

177. Y. Shen, J. Kuti, L. Lin and P. Rossi, in *Lattice 88*, Nucl. Phys. **B**(Proc. Suppl.) **9** (1989) 99.

178. A. Hasenfratz and T. Neuhaus, Phys. Lett. **B220** (1989) 435.

179. A. Hasenfratz, W. Liu and T. Neuhaus, Phys. Lett. **B236** (1990) 339.

180. I.-H. Lee, J. Shigemitsu and R. E. Shrock, Nucl. Phys. **B330** (1990) 225; **B334** (1990) 265; S. Aoki, I.-H. Lee, D. Mustaki, J. Shigemitsu and R. E. Shrock, Phys. Lett. **B244** (1990) 301.

181. M. A. Stephanov and M. M. Tsypin, Phys. Lett. **B236** (1990) 344.

182. V. A. Miransky, Nuovo Cim., **90A** (1985) 149.

183. K. Kondo, contribution to parallel session (paper #271–272).

184. S. T. Love, contribution to the parallel session (paper #213).

185. P. E. L. Rakow, preprint DESY-90-029 (1990).

186. E. Dagotto and J. B. Kogut, Nucl. Phys. **295** (1988) 123.

187. M. Okawa, Phys. Rev. Lett. **62** (1989) 1224.

188. A. Kocić, S. Hands, J. B. Kogut and E. Dagotto, preprint NSF-ITP-90-62 (1990) and references therein.

189. E. Dagotto, A. Kocić and J. B. Kogut, Nucl. Phys. **B331** (1990) 500.

190. S. P. Booth, R. D .Kenway and B. J. Pendleton, Phys. Lett. **B228** (1989) 115.

191. A. Horowitz, in *Lattice 88*, Nucl. Phys. **B**(Proc Suppl.) **9** (1989) 403; in *Lattice 89*, Nucl. Phys. **B**(Proc. Suppl.) **17** (1990) 694.

192. M. Göckeler, R. Horsley, E. Laermann, P. Rakow, G. Schierholz, R. Sommer and U.-J. Wiese, Nucl. Phys. **B334** (1990) 527; preprint DESY 90-085 (1990).

193. M. Lüscher, Nucl. Phys. **B341** (1990) 341.

194. The APE Collaboration, in *Lattice 88*, Nucl. Phys. **B**(Proc. Suppl.) **9** (1989) 562; F. Rapuano, contribution to the parallel session.

195. The QCD Teraflop project, S. Aoki, R. Schrock, C. Bernard, M. Ogilvie, K. Bitar, R. Edwards, U. Heller, A. Kennedy, D. Petcher, R. Brower, J. Potvin, C. Rebbi, F. Brown, N. Christ, R. Mawwhinney, C. DeTar, S. Gottlieb, I.-H. Lee, G. Kilcup, J. Shigemitsu, J. Kogut, A. Kronfeld, S. Ohta, D. Sinclair and A. Soni, presented by C. DeTar at the parallel session.